DUET
The Dual Use Exoplanet Telescope

Final Report
NASA Innovative Advanced Concepts
Phase I Study
Grant For Research 80NSSC19K0967

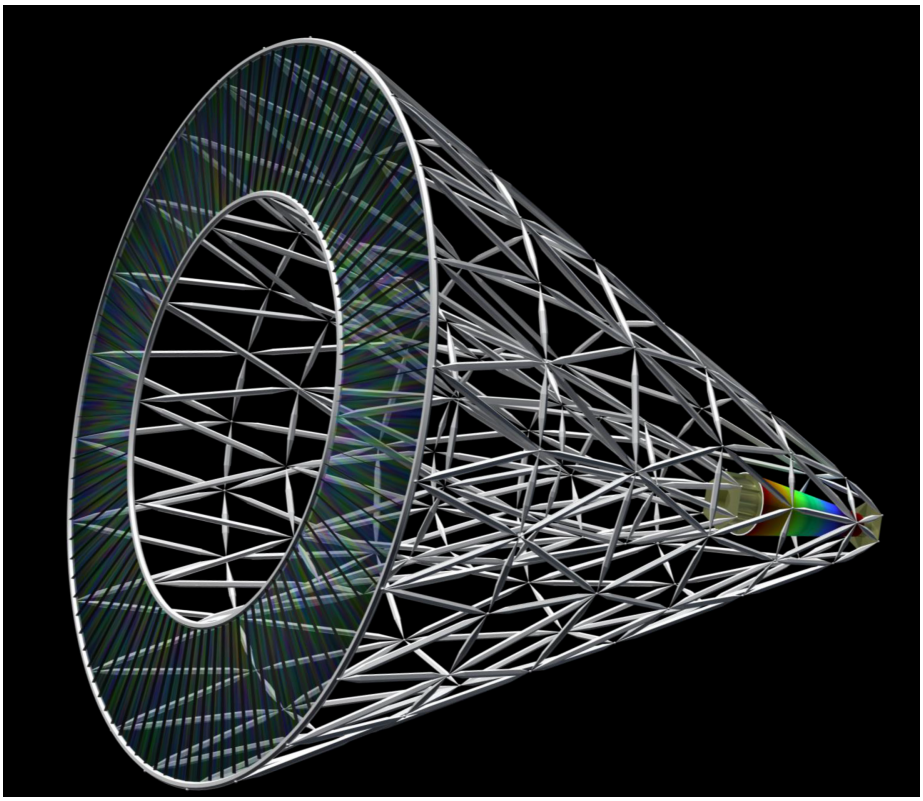

Thomas D. Ditto [1] (P.I.)
Mei-Li Hsieh [2], Heidi Jo Newberg [3], Robert Hoyt [4], Daniel Angerhausen [5]

March 9, 2020

[1] 3DeWitt LLC, Ancramdale, NY 12503-0010
td@3dewitt.com

[2] National Chiao-Tung University, [3] Rensselaer Polytechnic Institute
[4] Tethers Unlimited Inc., [5] Bern University

Table of Contents

List of Illustrations

Glossary of abbreviations

ADI – Angular Differential Imaging
CD – Compact Disc
CNC – Computer Numerical Control
ConOps – Concept of Operations
DARPA – United States Defense Advanced Research Projects Agency
DNA - Deoxyribonucleic Acid
DOE – Diffractive Optical Element
f-o-v – field of view
HOE – Holographic Optical Element
HST – Hubble Space Telescope
iSAT – in-Space Assembly Telescope
JWST – James Webb Space Telescope
mas - milliarcseconds
MOIRE - Membrane Optical Imager for Real-Time Exploitation
PBS – Prism Beam Splitter
POG – Primary Objective Grating
TRL – Technology Readiness Level
TUI – Tethers Unlimited Inc.
VPHG – Volume Phase Holographic Grating
WFIRST – Wide Field Infrared Space Telescope
Zemax – Trade name for the Zemax optical engineering program

1. Executive Summary

The Dual Use Exoplanet Telescope (DUET) is intended as a follow-up to surveys for exoplanets by making detailed observations of specific extra-solar systems. "Dual use" refers to a choice or combination of traditional Doppler shift spectroscopy used to make the first confirmed discoveries of exoplanets [1] and, on the other hand, spectrographic analysis of directly observed exoplanets, a type of observation not yet possible.

Exoplanet discovery missions are coming off the drawing boards faster than other space telescopes. [2] **Indirect** detection by stellar radial velocity is possible with astrometry.[3] However, Doppler shift from high resolution spectroscopy is not presently being pursued in any embodiment of space telescope known to us. Massive échelle spectrographs used for Doppler from the ground are not space qualified. **Direct** observation has led to a race for coronagraphy that can handle the 10^{10} contrast ratio of parent star to its planets. Nearby exoplanets are faint, nominally about 30th magnitude, and their orbits subtend just hundreds of millarcseconds (mas). While transit photometry permits brief partial direct observation of atmospheres (without albedos) during occultations of exoplanets orbiting in line of sight with us, 99% of exoplanets do not occult as seen from Earth.

In this exoplanet mission context, it is no surprise that space telescopes are seeking larger primary objectives to increase photon collection and angular resolution. "Bigger is better" is a mantra among astronomers. However, mirrors scale up in mass approximately as the cube of their diameter, and the largest and by far the most expensive telescope ever built, JWST at 6.5 meters, cannot equal a growing number of 10 m ground-based telescopes. A quantum leap to 39 meter diameter is now underway with the ELT. Size is not a problem once in orbit, but launch and deployment are constrained by mass.

DUET addresses spectrographic indirect and direct observation for exoplanet discovery at low aerial spacecraft mass. DUET can serve as the large diameter space telescope sought for exoplanet observatory missions. Our rethinking of telescopy comes from a paradigm shift after four centuries of lens/mirror tradition. We place the burden of photon collection and resolving power on diffractive optics which are both low mass and spectrographic. Our studies [4] have indicated that transmission diffractive optical elements (DOEs) are an alternative allowing new types of coronagraphy, very high resolution spectroscopy, launch mass reduction and in-space assembled telescopes (iSATs).

1.1 The Impetus

In the 400 years of telescope-assisted modern astronomy, definitive proof of the existence of planets outside our solar system was elusive despite the logical inference dating back to Giordano Bruno's assertion predating telescopes that one would expect to find them. A highly accurate spectrographic telescope was needed for the first incontrovertible proof. Once the confirmation was made, a sensitive photogrammetric survey, Kepler, revealed that exoplanets were abundant. Statistically one would expect to discover some with earth-like features, but better telescopes for the search are needed, because the complex characteristics of Earth 2.0 are not readily observable with any existing telescope.

In a world of eight and ten meter ground telescopes, Hubble showed what a two meter space telescope could do, and it is fair to assume that a 6.5 meter JWST will do its share of breakthrough astronomy in some ways matching the 39 meter ESO ELT.

The question we asked was "Why are space telescopes smaller than ground-based ones?" Arguably space deployment is more demanding than the ground, even if compared with the rigors of mountain tops. However, the zero-g environment must be factored into the issue of scale. To make a biological comparison, whales in the buoyancy of water have evolved in sizes well beyond pachyderms whose bones must resist gravity.

Our proposed solution to the space telescope scale problem came with the serendipitous outcome that a flat gossamer membrane primary objective is intrinsically spectrographic. Since Fraunhofer noted the similarity of stellar spectral lines with those of the Sun, it has been axiomatic among astronomers that "A spectrum is worth 1,000 images." Our idea was to model a very high resolution spectrographic telescope capable of discovering Earth 2.0 from a space platform.

1.2 Result

Our nine month investigation confirmed that a point source polychromatic source, in effect a simulated star, can be magnified with a circular primary objective grating (POG) into a target-shaped spectrogram. NIAC support allowed us to set up a precision optical bench to realize a refined version of an image that we had primitively realized years earlier when first submitting a NIAC Phase I proposal. Our expectation had always been that a circular primary objective grating (POG) that was perfectly co-axial with a source of illumination would produce a uniform circular spectrum. It does, Figure 1. The source was a 25 μm spatial filter pinhole. A circle of 5 cm diameter can be seen at 594 nm. The effective magnification is 2,000.

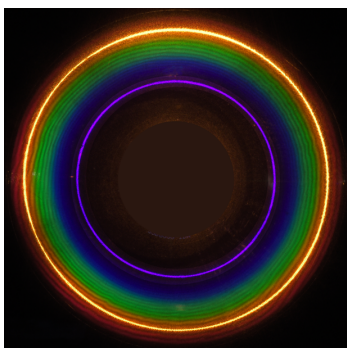

Fig. 1 Circular spectrogram

Astronomical telescope magnification is limited by aperture and collection area. The former parameter is also affected by wavelength. In the example of Figure 1, a 405 nm violet circle uses less of the POG than the longer 594 nm yellow line. Violet magnification is also less, 1,600 times. If the frequency of the lines on the POG were to increase, violet spectral spread would increase proportionately. This allows us to tailor a POG for a spectral band being observed. None of this is outside prior teaching in optics.

Circular POG spectroscopy is a novelty in astronomical telescopes. Because the primary objective is highly chromatic following the diffraction equation, the "bug" that Newton removed with his universally adopted achromatic mirror may turn out to be a "feature" when the goal is the take precision spectrograms. For example, in Doppler shift measurements to detect direction and radial velocity, precision of 5 cm/sec will allow indirect detection of Earth 2.0 candidates at any distance where signal to noise allows measurement of absorption lines of the host star. Such sensitivity to spectral shift can be obtained with a spectrometer featuring a grating of two meters or greater. DUET might have a primary made from a 10 meter ring on a 50 meter annulus. The resulting power might not only reveal radial velocity but possibly stellar acceleration, a measurement that today requires multiple visits to a target under study. Beyond our stated purpose of exoplanet detection, such a feature would have utility in the study of Dark Matter.

Direct observation of an exoplanet requires the removal of the glare coming from the host star. Our investigation led to the invention of three novel coronagraphs unique to a highly chromatic circular spectrogram. Angular Differential Imaging (ADI) has been practiced with mirror telescopes, but circular images separated by spectral lines allow a symmetrical removal process. In Phase I we demonstrated this on the bench, Figure 2.

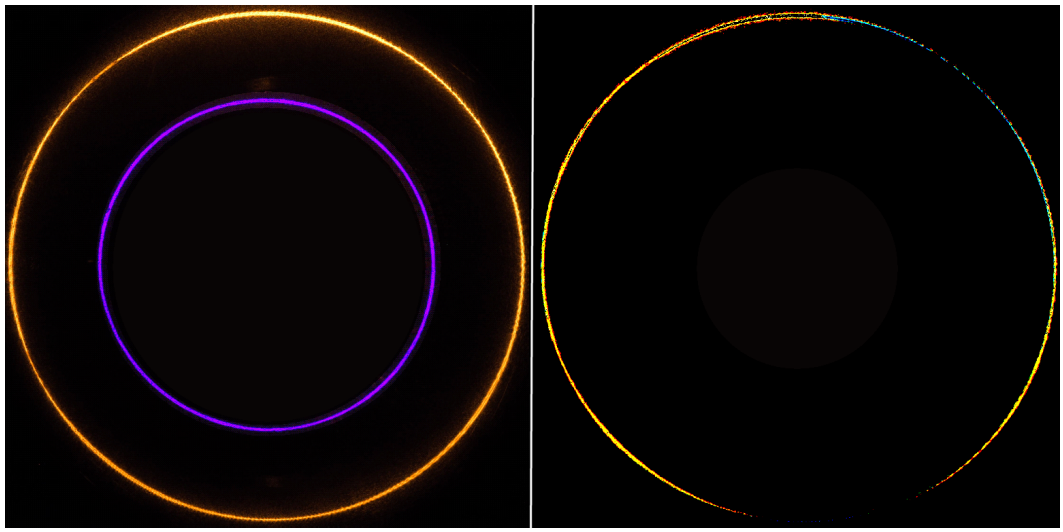

Fig.2 ADI subtraction of 405 nm line of "star" leaves 594 nm "exoplanet" line

Here the yellow line was offset to simulate the 140 mas angle subtended by Earth's offset from the Sun. The subtraction of an on-axis 405 nm line from the "Sun" left a recovered yellow 594 nm line from the "Earth 2.0."

In addition to ADI, in Phase I we invented two more coronagraphic methods that exploit very high resolution spectroscopy. One exploits shifts of spectral lines found in exoplanet albedos. A third, BLOC (Bifurcated Light Optical Coronagraph) performs interferometric nulling in a manner that attenuates the star but causes no other fringes, Figure 3. BLOC creates an optical "singularity" null out of polychromatic light that is split in a fiber and then recombined. Equal but opposite spectra then are symmetrically opposed in a unique dual mirror spectral interferometer. [5] Zemax was used to model BLOC. A bench version will require fiber optics that are listed to be developed in Phase II.

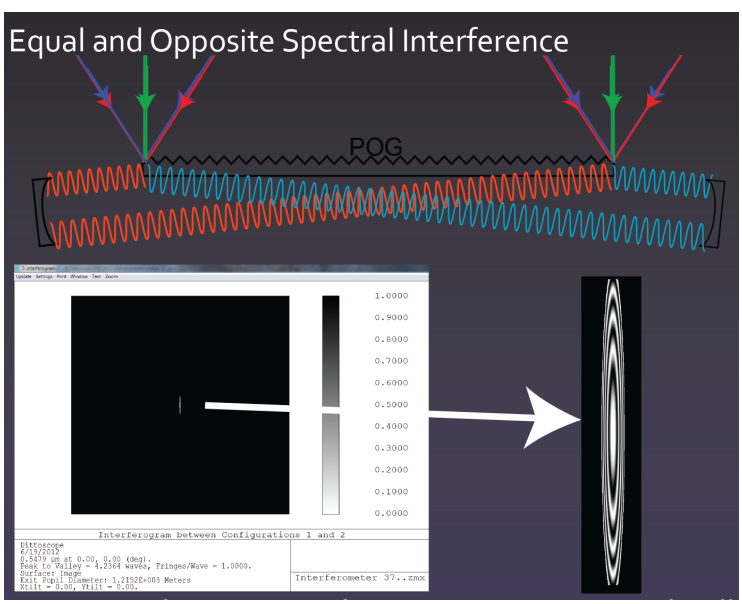

Fig. 3 BLOC knocks out the parent star but not its exoplanets

The sizeable POG proposed for DUET is a Gabor Zone Plate (GZP) in the form factor of an annulus. A GZP was modeled in Zemax and made on the bench by analog holography in a photopolymer. It performed geometrically as predicted focusing a broad band plane wave at focal lengths proportional to wavelength. A follow-up Zemax model included the spectrographic secondary, holographic optical elements (HOEs) that focus, Figure 4.

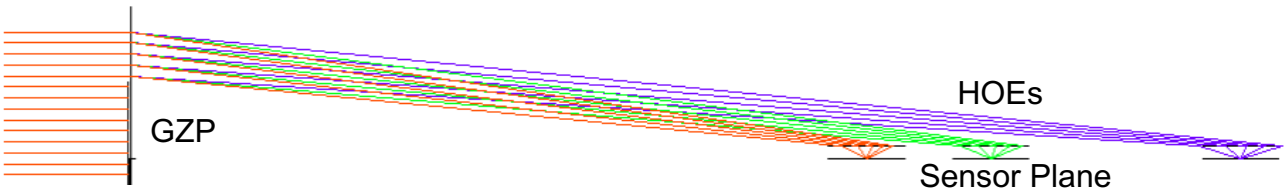

Fig. 4 Zemax model of HOEs that redirect the spectrum down to focus on to a sensor plane

The most vexing optical problems might seem to be solved in Zemax or on a bench top, but putting DUET into space calls for ConOps that account for launch of a 50 meter scale POG. The solution we have been exploring is iSAT (in-Space Assembled Telescope). Unlike mirrors, the GZP annulus can be rolled up on a mandrel. Its 10 meter width is then compatible with such lifters as the Falcon 9 Heavy. A stowage configuration under a fairing for all in-orbit components was diagrammed, Figure 5. Once in orbit where micro-gravity presents no obstacles to structural integrity, the gossamer primary objective can be unrolled along a track, Figure 6. ConOps are the work product of Seattle-based Tethers Unlimited Inc. (TUI). In TUI we truss.

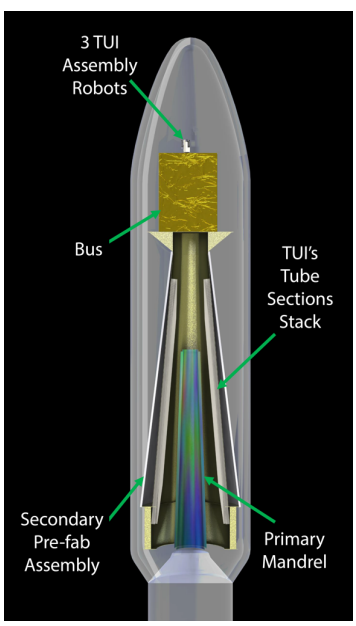

Fig. 5 Launch Payload

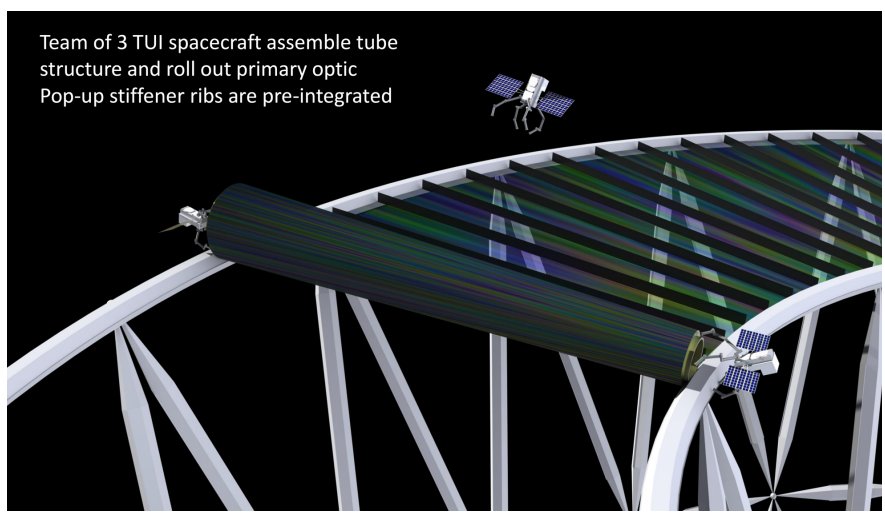

Fig. 6 iSAT process for a 50 meter version of DUET with a 10 m ribbon. TUI innovation of stiffeners pre-integrated into the stowed mandrel provide structural integrity trusswork and tensioning for the optical membrane. The robots are a variation on the NIAC-developed spider-bot.

Phase I confirmed anticipated geometric optics. The low areal mass of membrane DOEs suggest that with iSAT construction DUET and related telescopes can achieve greater apertures and collection areas than ground-based telescopes. However, unresolved questions about efficiency of these optics must be addressed during Phase II.

2. Background

2.1 How do we observe exoplanets?

Hans Lipersky's 1608 "spy glass" was immediately recognized as the solution to optical magnification of objects at a distance. This was fine for a sailor, but the astronomical telescope was born when Galileo used it to study the sky. In a similar manner, our innovation will serve science if our project demonstrates astronomical utility. We have designated discovering exoplanets as a target application, and we seek to demonstrate in the lab that DUET is a means to find habitable worlds by running lab experiments that simulate finding Earth 2.0. We won't be discovering the moons of Jupiter as Galileo did, but we have identified a feature of Earth's albedo that gives us a meaningful benchmark.

Today, the astronomy community focus is on observations of atmospheres of rocky planets of main sequence M-class stars which are the most numerous within 10 pc, i.e., our "neighborhood." Because M stars are relatively faint, their census is in-progress, Table 1. [6]

Census year	2000	2010	2018
white dwarfs	18	20	20
O stars	0	0	0
B stars	0	0	0
A stars	4	4	4
F stars	7	7	7
G stars	19	19	19
K stars	44	44	44
M stars	**198**	**340**	**378**

Table 1 Our stellar neighbor population

M stars offer several observational advantages. Compared to more massive stars, transits of (potentially habitable) planets around M stars are more numerous and deeper. Radial velocity observations benefit from the proximity of the orbiting planets. M star secondary eclipse measurements offer higher contrast ratios. Therefore, current surveys are not only working on a comprehensive, growing census of M-class stars but are also actively searching for transiting planets around these hosts [7] [8] [9] They will be targets for IR atmospheric characterization by JWST during transits – made possible because coronagraphy is not required. JWST does spectroscopy well but not exoplanet coronagraphy. WFIRST will have a coronagraph designed for direct exoplanet observation but less angular resolution, a 2.4 m mirror compared to JWST's 6.5 m mirror.

Despite observational advantages on M-stars for conventional telescopes, the question of the actual habitability of planets around M-dwarfs is one of the most debated and a topic of high scientific interest in the exoplanet community at the moment. [10] High stellar activity of the host stars, high levels of X-ray and UV radiation and the likely tidal locking of planets in their habitable zone may pose insurmountable problems for the origin and persistence of life in these circumstances. Arny [11] argues that K dwarf stars are a better target for remote detection of biosignatures on directly imaged exoplanets, because ionizing radiation on dwarf K stars occurs over a shorter star lifetime than on the more numerous M-class stars. He simulates spectra in the infrared and ignores the near-UV, basing observational goals on absorption lines that are signatures for biogenic gases.

Admittedly, UV sterilizes and would not foster life. However, if Earth is nearly unique as an incubator for DNA, the 19 sun-like G-class stars in our neighborhood bear special scrutiny even though they emit in the UV. A non-intuitive argument may come down to the very presence of UV in the parent to foster life on exoplanets. Earth has life.

Our observational strategy is based on a unique property of our "pale blue dot." It turns out that Earth is not pale in the near-UV but rather surprisingly luminescent, (Figure 7).[12] Clouds and the ocean increase in brightness at shorter wavelengths as the Sun loses flux in the same band. This stands in contrast to every other planet in our solar system, even the blue ones: Neptune and Uranus. see Figure 8. Venus which is yellow, as well as Neptune which appears purple, decrease in flux and follow the solar spectrum in the UV.

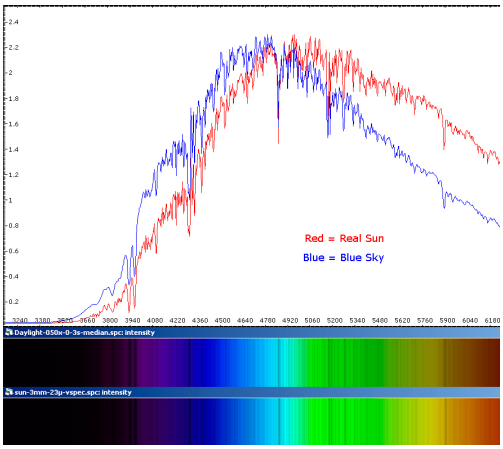

Fig. 7. Earth shifts energy from the solar spectrum into the near-UV

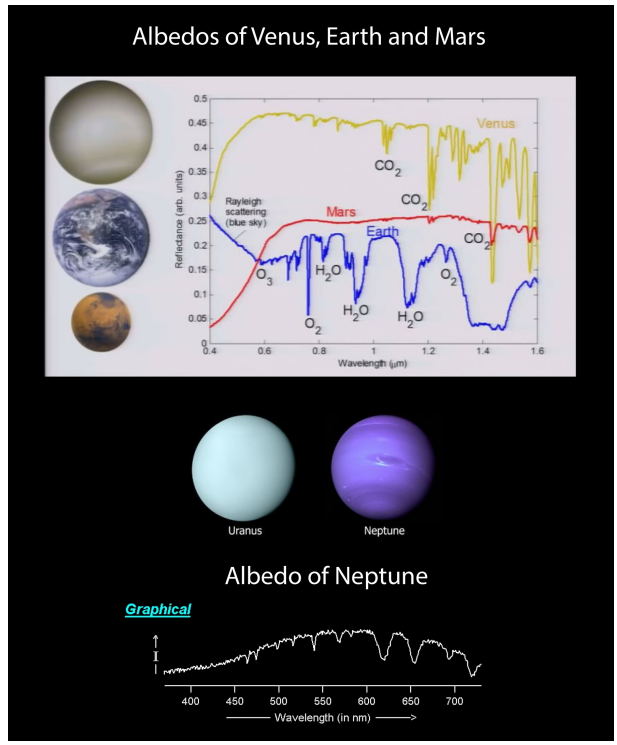

Fig. 8 Our Solar System Planet Albedos

Compared to all other planets in our solar system, only Earth gains in albedo where our Sun decreases in flux in the near-UV. The reason Earth is luminescent is attributable to the sum of Rayleigh scattering in the upper atmosphere and longer wavelength absorption in the oceans. These are signals in the search for habitability. First, we are looking for water exoplanets. Secondly, the Rayleigh scattering is one of the Earth's shields, along with such things as the magnetosphere, that keep our DNA from ionizing.

We can use this phenomenon in an experiment that will qualify DUET for detection of Earth 2.0. The source illumination for our bench test will have a 5500° K black body source modeled on the Sun with near-UV lines for Earth's albedo. The same experiment can also show how we use stellar absorption lines to lower contrast and how ADI as a coronagraph can be used with GZP primary objectives.

HOEs are less efficient than mirrors. Our roadmap to making a convincing demonstration of DUET will be to show that HOEs are capable of capturing enough light at full scale to resolve 30th magnitude objects, at the very least in the 100 nm wide broad bands that fit our proposed Earth 2.0 observational strategy.

2.2 Primary Objective Grating (POG) telescopes

The benefit of a diffraction grating primary objective has been studied by the Mendels, Hyde, Andersen, and others over the past quarter century, [13] but their designs looked insufficiently to the architectural feature that made the 17th century refractor and reflector possible, the secondary optics. Diffraction primaries were shown to provide an orders-of-magnitude reduction in areal mass over mirrors, but bandwidths were extremely narrow and at inconveniently long focal lengths – much like the discontinued refractors of yore.

Notable in its pursuit of a diffraction primary was the DARPA-funded MOIRE project [14] which originated in a series of experiments and papers by Geoff Andersen [15] and was pursued under contract by Ball Aerospace. The name could be regarded as a misnomer, because the abbreviation MOIRE stands for "Membrane Optical Imager for Real-Time Exploitation," which has nothing to do with "Moiré" in mathematics and graphics.

What was wrong on MOIRE's practical side was the notion that a POG telescope would work almost exactly like a classical refractor, focusing light on a secondary transmission optic that formed a 2D image on a sensor. By the very definition of an HOE, the image had to be restricted to a monochromatic band. To broaden the bandwidth Andersen describes a secondary with a pair of opposed mirrors that corrected a custom DOE. [16] This approach improves the extremely narrow bandwidth to as much as 70 nm, according to DARPA, but in his published paper (and in private conversation with Ditto) Andersen expected no more than a diffraction-limited bandwidth of 40 nm.

As it happens, dispersion in refraction spreads a spectrum in the opposite sense as diffraction, so the two aberrations, being opposite, can conceivably cancel themselves out. We investigated an optical train that refocused an HOE, similar in its variable frequency to the MOIRE POG. An intermediate refractive element is used to compensate for wavelength dependent focal lengths of the holographic primary objective. [17]

Plastics have relatively high index of dispersion that might be used in a POG telescope secondary for correction of chromatic aberration. An example of dispersion by a plastic lens is shown in Figure 9. The central blue disk is ringed by colors of increasing wavelength which have proportionately lower angles of dispersion. We modeled a short focal length lens in Polystyrene which can be found in the Zemax miscellaneous glass catalog. The choice of the focal length is driven by the need to maximize the chromatic aberration of the lens. The focal length was not so much to increase magnification as to decrease chromatic aberration. A short focal length introduces pronounced aberration.

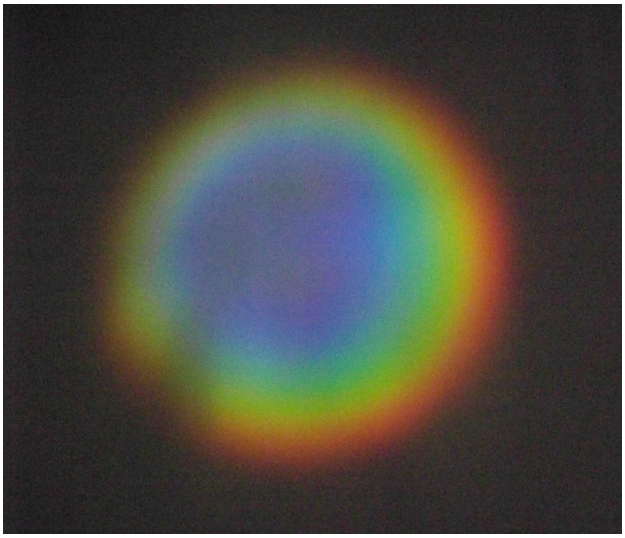

Fig. 9. Dispersion by a plastic lens

In the Zemax model, Fig. 11, the HOE is 80 mm in length. The effective focal length at 405 nm is 575.89 mm. The plastic lens is placed at 290 mm from the center of the HOE inclined at 80° relative to the HOE surface normal. It is 6 mm in diameter with a focal length of 9 mm at 405 nm. The embodiment of Figure 10 is a slitless spectrometer.

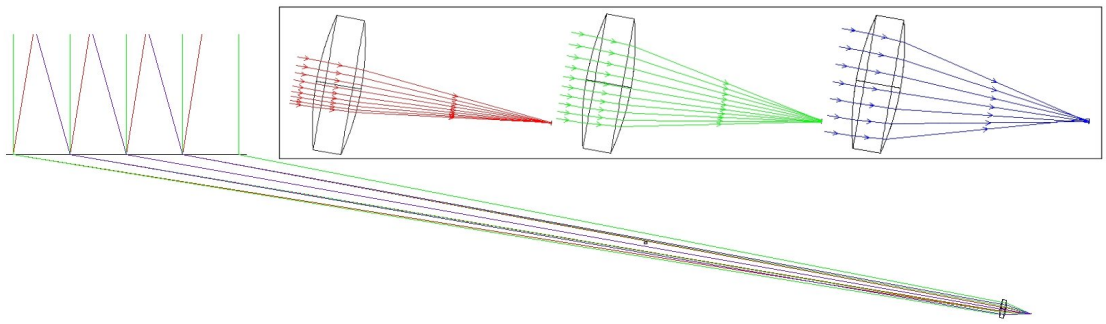

Fig. 10. HOE of focal length 576 mm with plastic lens of focal length 9 mm is used to correct chromatic aberration. Insert shows lens acting on red, green and blue wavelengths.

Slitless spectroscopy has been practiced in astronomy since the 19th century. A prism or a grating is placed in front of either a lens or mirror telescope. Each source then produces a spectrum. If the sources are sparse, their resultant spectra do not overlap ambiguously. However, even in sparse fields, trades are that short spectra are not detailed and exhibit overlapping higher-orders. Also, backgrounds are superimposed on top of each spectrum, lowering signal to noise. [18] Slitless spectroscopy has been employed on edges of objects such as the limb of the sun during an eclipse or as a primitive form of multiple object spectroscopy. The method is used on HST[19] and is anticipated for WFIRST.

It takes a secondary optic to disambiguate a wavefront from its primary objective. In the 17 th century compatible lens or mirror secondaries were the breakthrough that made the refractor and reflector telescopes possible. The primary formed a real image. The secondary lens or mirror then allowed the eye to see the image formed by the primary.

Diffraction gratings did not exist at the time. However, Newton did show that a spectrum dispersed from a prism could be resolved as a single color at a single angle with a secondary prism.[20] He did not think of his dual dispersion architecture as a form of telescope, but if the analysis of spectroscopy had been known back then, he might have.

Our innovation dating to 2000 is not far removed from Newton's famous double prism experiment of 1666. A secondary grating is used to extract a coherent spectrum from the overlapping spectra formed by a POG illuminated along the line of right ascension of an astronomical telescope. Unlike Newton's prisms, today we have powerful gratings that can stretch a single source from a point into a broad spectrum. The magnification can be by a factor in the tens of thousands. The embodiment using a plane grating as the POG is the sky survey instrument illustrated in Figure 11. Since 2002 have published over a dozen papers on this plane grating primary objective configuration.[21] and continue to investigate its potential as a survey telescope, most recently as ground-based near-earth object warning system.

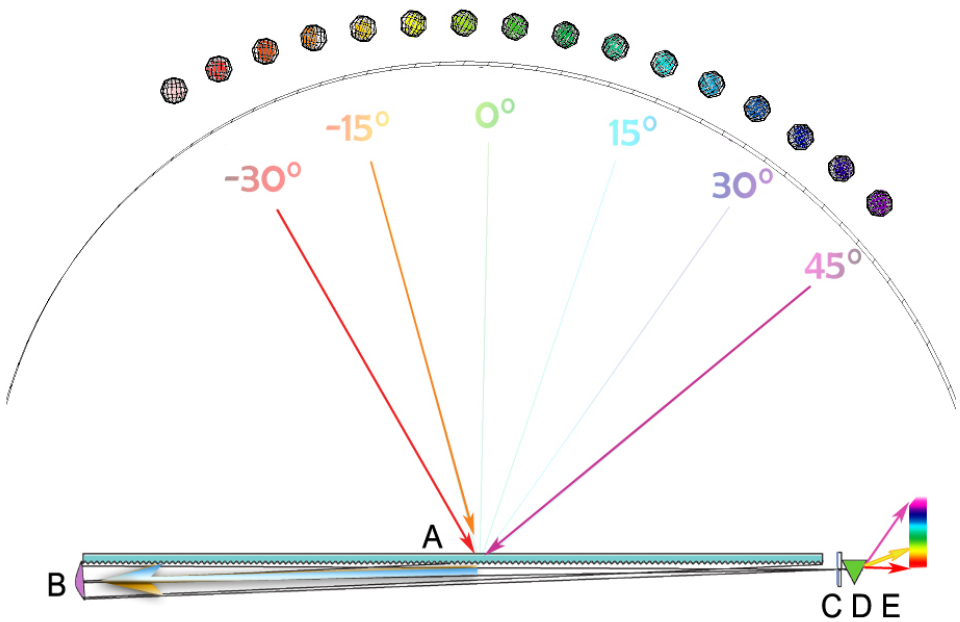

Fig. 11 A star in transit is diffracted by grating **A** at grazing exodus to secondary parabolic mirror **B**. Light is focused on slit **C**. A secondary disperser, **D** separates out all the visible objects as spectrum **E**. Three distinct angles -30°, -15°and 45° are illustrated in bold lines, but the entire line of right ascension is covered. In the course of an observation cycle, spectrograms are taken over all wavelengths for all stars.

The POG of Figure 11 has power only in one direction along the diffraction axis where an incoming plane wave is compressed anamorphically. Magnification in that dimension is determined by the length of the grating, that is, the length of POG **A** divided by the diameter of the secondary mirror **B**. On the other hand, in the lateral dimension the diffraction limit is determined not by the POG but solely by the diameter of mirror **B**.

Note the wide arc subtended in the diffraction dimension. Since the power of the POG itself is restricted solely to the direction of dispersion by diffraction, the étendue AΩ (collection area multiplied by product of the angles on the sky) grows as a linear progression, but the configuration yields a numerical étendue orders of magnitude greater than any other telescope.[22] This is a figure of merit for survey telescopes. However, this is somewhat an apples to oranges comparison, since the angle on the sky is correlated to wavelength, whereas a photogrammetric survey telescope such as the Vera Rubin survey telescope (formerly the Large Synoptic Survey Telescope), takes in all wavelengths all-at-once of any resolved object. However, the Rubin has no spectrometer nor could it. Since the POG is dispersive and the secondary is a spectrometer, the POG telescope is intrinsically spectrographic. The configuration of Figure 11 projects a spectrum onto the sky, and the spectrum of any one object is collected temporally as it drifts across through the f-o-v. We have estimated that a telescope like that in Figure 11 with a 100 x 1 m POG can take in a million very high resolution spectrograms in a single night of observation.

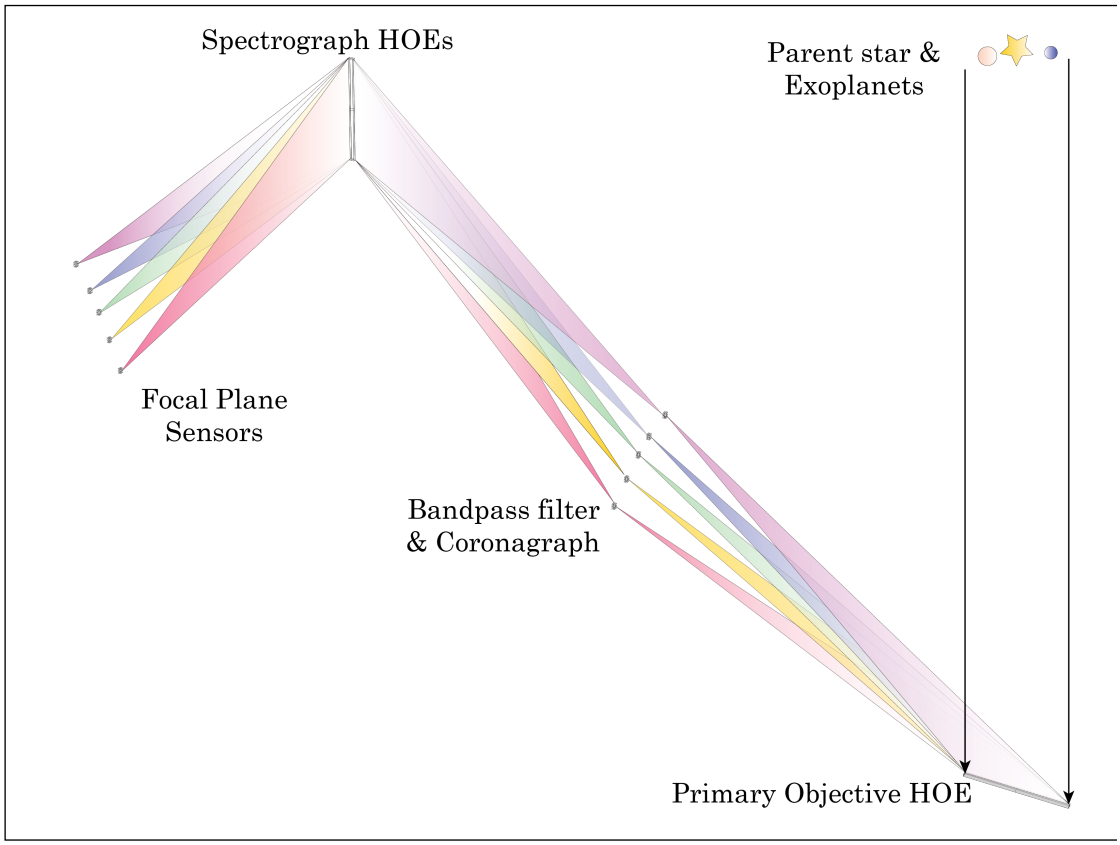

Fig. 12 HOMES – Holographic Optical Method for Exoplanet Spectroscopy

A linear ribbon form factor of the plane grating primary was applied to a chirped frequency grating, modeled as an HOE, that varied in pitch, Figure 12.[23] With an HOE as the primary, the field-of-view (f-o-v) can be restricted to a collimated angle on the sky, allowing the telescope to acquire sources within a narrow search area. An explicit purpose was to enjoy angular resolution sufficient to isolate exoplanets from each other and their parent star. As modeled in Zemax, the concept worked geometrically, predicting better than 1 mas resolving power with a 50 m primary. However, the leverage of the considerable length of the POG being only in one direction, the other dimension resolved no better than an arcsecond. The asymmetry did not lend itself to searching over any more than a narrow sliver of the exoplanetary system returning images of the exoplanets when they happened to line up with the ribbon-shaped POG.

2.3 Exoplanet Detectors – Special issues

Exoplanet detection represents a daunting but unavoidable challenge to astronomical instrumentation. [24] Aperture and collection areas of space telescopes must exceed the dimensions of legacy and near-term missions to provide the resolution and sensitivity requisite for discovery of Earth analogs in our stellar neighborhood. The diffractive primary objective telescope may provide a pathway, but it has its own issues.

2.3a Contrast

Exoplanets are faint. An Earth twin at ten pc is nominally 30th magnitude. Photons in the visible spectrum arrive here approximately at the rate of one per square meter per minute. Galaxies in the Ultra Hubble Deep Field were about as faint. Integration time to record the Deep Field image with a 2 m mirror amounted to over 11 days.[25]

An abiding obstacle to the development of the POG telescope is not its potential diameter but the limited efficiency of diffraction gratings. Incident energy is distributed into the zero-order and the higher diffraction orders. MOIRE was reported testing at 0.4% efficiency in one order with a theoretical limit of 3%.[26] A subsequent independently pursued experiment with a modification of the MOIRE photon sieve reported 12% efficiency. [27] In astronomy throughput losses are problematic.

That said, the size of the "bucket," that is, the collection area can mitigate losses to the zero-order. Unlike mirrors, the POG is a flat surface which using embossing methods in plastic arguably can be minted into deliverable kilometer scale primary objectives with collection areas in the thousands of square meters. In an embodiment of the plane constant pitch POG as illustrated in Figure 11, we have shown that the collection can be made on both sides of the POG, Figure 13, essentially doubling collection. By selection of a sub-wavelength pitch, diffraction is almost entirely in the first-order. This does not suppress losses to the zero-order but limits losses to orders above the first-order.

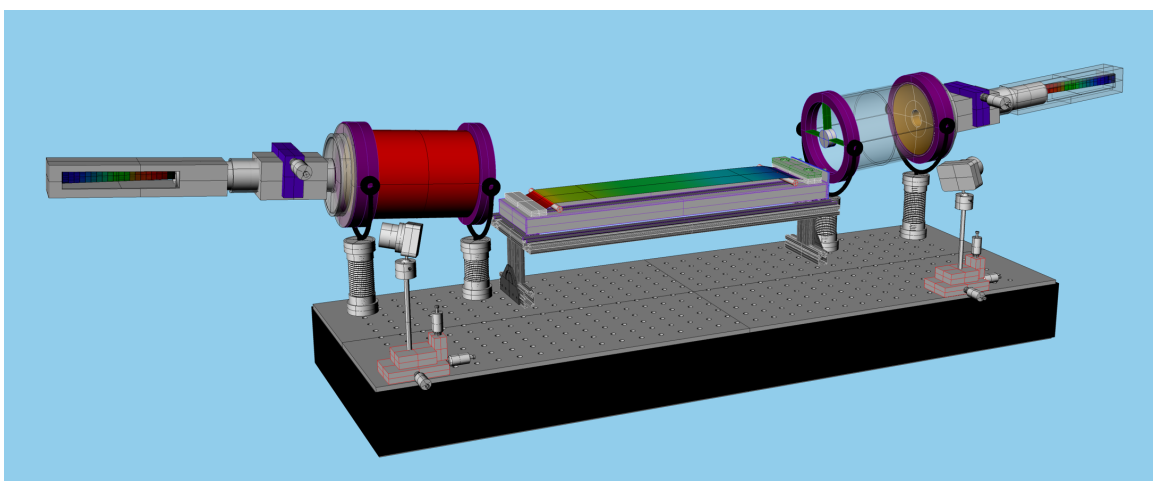

Fig. 13 Dual secondary spectrographic telescopes share a common POG

When the target is faint, a single wavelength band as narrow as the POG can resolve may not capture enough light to produce any signal above noise. Extraordinary spectral resolution works against the goal of seeing in darkness if the sensor is photon starved. A solution is to bin refined wavelengths into fewer bands. On the other hand, the parent star will be producing 10^{10} more photons than its exoplanets, and here the exquisite spectral resolution can be useful, for example, to take radial velocities. We will also show in this Report that fine spectral bands offer a unique approach to a type of coronagraph that subtracts out the star's flux, leaving behind traces of its very faint exoplanets.

2.3b Angular resolution

The spectral resolution of a POG is proportional to its length. Just as mirror telescope resolution is diffraction limited by mirror diameter, POG resolution is limited by POG length and wavelength; λ/D resolution is λ/L where L is the length of the grating.[28] See Figures 14-15. Similarly, as focal length does not change the limitation in resolution of the mirror telescope, groove to groove pitch length does not change the limitation of resolution of a POG. We anticipate sub-wavelength pitch on our astronomical POG, because losses to higher-orders are mitigated, but long pitch length échelle spectrographs demonstrate that when there are benefits to using many higher-orders when taking a spectrum, spectral resolution is preserved. In the final analysis, length sets resolution.

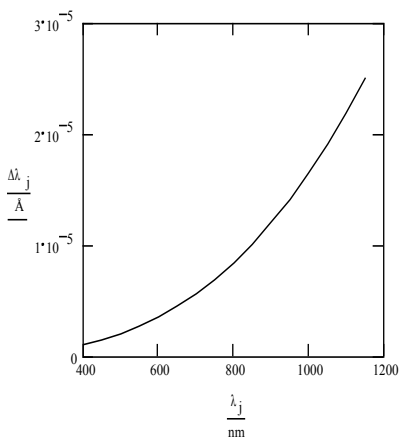

Fig. 14 Spectral resolution in Å

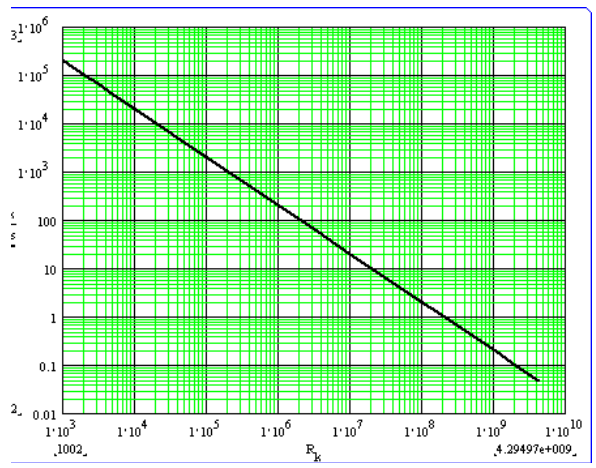

Fig. 15 Δi mas as a function of resolving power R

If perfectly ruled on a perfect surface, grating resolving power R is directly proportional to grating length and inversely proportional to wave length L where angle i is the incident angle and angle r the angle at which the light is collected.

(1) $$R = L\frac{(\sin(i)+\sin(r))}{\lambda}$$

Contemporary large grating spectrometers such as the HIRES spectrometer on Keck I boast resolving powers approaching six figures, and this has been deemed a practical benchmark, since HIRES can measure the Doppler moments for radial velocities of stellar spectra in meters/sec. By way of contrast, gratings of kilometer length would have theoretical resolving powers in nine figures. In Figure 15 we graph the theoretical spectral separation possible with a kilometer length grating of 1650 lines per mm (p = 606.06 nm) in the spectral range recorded by garden variety silicon photodiodes.

A POG telescope differs from prior art in that it produces spectral dispersion in proportion to its angle on the sky. Solving (1) for the incident angle:

(2) $$i = \arcsin\left(n\frac{\lambda}{p} - \sin(r)\right)$$

Theoretical resolution limits in mas can be seen in Figure 16. Angular resolution is sufficient to separate a neighboring exoplanet in an orbit comparable to Earth.

Compared to mirrors where three dimensional curved figures must be held to λ/4 to achieve the diffraction limit across their considerable diameter (100 nm error for visible), gratings are not only flat, but their surface flatness tolerances are considerably relaxed.

For any angle of incidence i there is a superimposed image from $i + \Delta\alpha$, and the difference forms the error Δi. Consider:

(3) $i_2 = i_1 - \Delta\alpha$

(4) $r_2 = r_1 - \Delta\alpha$

Solved for λ in the first-order we obtain a new wave length received as a result of the imperfect grating.

(5) $\lambda_2 = (\sin(i_2) + \sin(r_2))p$

For any λ there is an error

(6) $\Delta\lambda = \lambda - \lambda_2$

Figure 16 is a graph of Δλ as a function of λ for the grating with one micrometer unevenness over 100 m when r_1 is 78°. The angular error is shown in Figure 17.

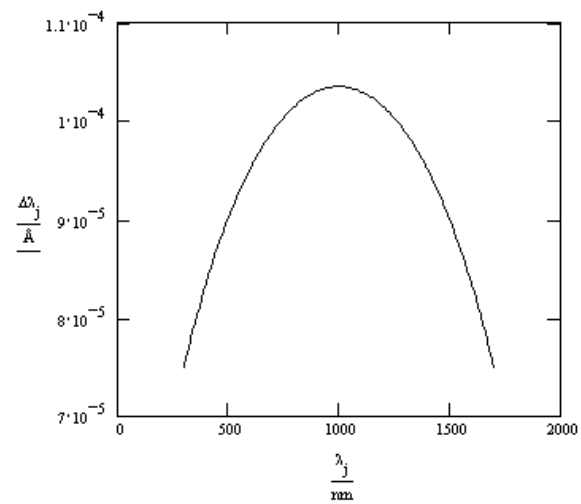

Fig. 16 Chromatic aberration at r=78°of a optical flat uneven to 1 μm/100 m

The angular resolution that can be reached is determined by the difference of the angle as determined by Equation (6) the error minus the same angle without the error.

(7) $$\Delta i = \left(\arcsin\left(\frac{(\Delta\lambda + \lambda)}{p} - \sin(r)\right) - \left(\arcsin\left(\frac{\lambda}{p} - \sin(r)\right)\right)\right)$$

The examples given are for a case where observations are in the 300 to 1800 nm band. The calculations predict that a POG is robust with respect to the flatness of the grating surface.

Creation of large flats might be less of a problem in fabrication than manufacture of very large telescope curved surface reflectors.

In contemporary practice, very large telescope curved surfaces are generally an array of mirrors that must be aligned with each other over the larger surface. JWST uses pistons to actively adjust the segments in order to eliminate interstitial lines and maintain optimum curvature. Alignment of flat surfaces with each other to the precision of the grating lines may be more practical.

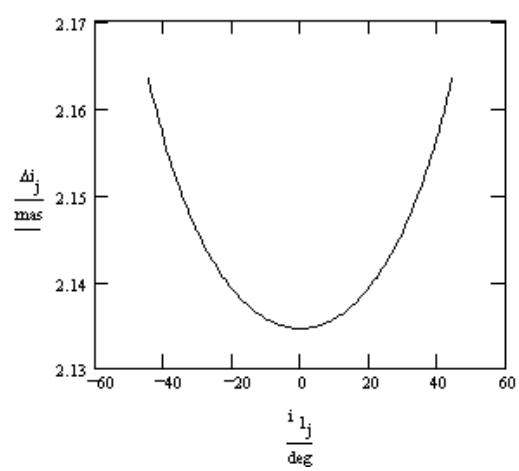

Fig. 17 Angular Resolution using flat of Fig. 16

3. DUET Concept

Duet is an astronomical telescope without mirrors or lenses. The choice of using flat gossamer membrane optical surfaces is motivated by the need to break with conventions that have restrained space telescope diameters to less than those found on the ground. The performance objectives that fall out from the diffraction optics are a consequence of the behavior of light in the diffraction grating regime. Prior to DUET, we developed THE MOST, The High Étendue Multiple Object Spectrographic Telescope, a survey telescope that would catalog all stars in a line of right ascension. Now, we are acting under the presumption that candidates for follow-up have been selected.

3.1 Single stellar system isolation

A spectrogram can be recorded with a telescope that has a f-o-v much wider than the virtual point source of a single star. A mask cuts out competing sources of illumination. Almost never would there be a presumption that the star can be directly imaged over the star's considerable diameter, because mirror diameters are too narrow to resolve such a distant image. In part, this is why spectrograms are valued, because they expand a point into a line of considerable length from which data about star chemistry and movement can be extracted.

Our approach is to convert a wavelength into an angle on the sky. The POG creates overlapping lines of color from every source to strike the grating. To discriminate each division of arc on the sky, a precise wavelength band is assigned to each pixel in the secondary. If a secondary sensor receives any light at an assigned wavelength band, the source must be from its restricted set of incident angles on the sky. It is axiomatic to our approach that an off-axis source can be filtered out because it will diffract at non-competing wavelengths when compared to the specified angles and correlated wavelengths of the single stellar system being studied.

3.2 Spectral Doppler Shift

DUET has two uses, and one of them is taking radial velocities by the Doppler shift of the wavelengths of light in the line-of-sight from the telescope. This effect is most pronounced along the line-of-sight, but a transit is not necessary to see a star's direction of movement. The observation is indirectly affected by gravitational forces exerted by exoplanets on their parent star.

Past observations with échelle gratings reaching $R > 60{,}000$ have achieved radial velocity measurements in the m/sec range. An Earth 2.0 in the habitable zone of a G-Class star in our neighborhood can be detected in the cm/sec range. This order-of-magnitude increase in sensitivity is ultimately limited by the length of the diffraction grating.

DUET is presumed to have an annulus ribbon of 10 m (over a ring diameter that may be in a 30 to 100 m range). This compares with ground-based échelle spectrographs that may be a meter long. Two meter spectrographs are coming on-line in the pursuit of an Earth 2.0 indirect detection. If DUET's spectrographic resolution is in the ballpark of an order-of-magnitude more precise than existing ground-based spectrographs, then it follows it can compete to take Doppler shift reading sensitive to Earth 2.0 exoplanets.

3.3 Direct Observation

The idealized DUET observation is not a "photographic" image of an exoplanet but rather its spectrographic signature. If an exoplanet is seen as a pixel or possibly several pixels, it presents the same problem as taking direct images of stars. They are effectively points in so far as the resolving power of a telescope is concerned. However, a star spectrum carries detailed information on star chemistry and motion within its spectrum.

The aperture needed to form a "photographic" image of an exoplanet would be on the scale of many kilometers. To create an image with the pixel equivalent of images we have of solar system planets, the telescope's primary objective would have to be on a unrealizable scale with contemporary or near-term optics. Only a group of space telescopes flown with precision over kilometer distances between them would have the resolution we are familiar with in local solar system planetary observation.

The possibility exists for widely separated optical telescopes to combine their data. A synthetic aperture interferometric method has been studied for NIAC by Jordan Wachs of Ball Aerospace. [29] A constellation of DUET type telescopes might perform the observations that Wachs describes. With DUET, Wach's interferometer would have a complete spectrum, filling out the channels covered by a local oscillator frequency comb as well as increasing the size of the bucket from 1.5 m diameter used in his calculations to a collector area greater than 500 m^2. He does consider a narrow bandwidth POG telescope modeled on MOIRE to increase the size of the collector, [30] but MOIRE limits photon collection, because its architecture intrinsically results in a narrow bandwidth and it has very low efficiency, as we discuss in Section 2.2 above.

If an exoplanet is at 30th magnitude, even large diameter telescopes do not receive enough photons to assemble detailed spectra that might reveal subtle absorption lines of biogenetic material, notwithstanding that libraries of these signatures exist when taken with the convenience of an Earth laboratory. DUET distributes its spectra around a circle, the resulting circumference further starving its sensors of photons. An example of the raw image that might be collected is illustrated in Figure 18. These detailed spectral lines must be binned from photon counters into a few broad bands to ascertain the presence of exoplanets. It is likely that instead of resolving 1 to 10 nm lines widths, DUET will struggle to resolve 100 nm bands. That said, if exoplanets are observed, the "single pixel" will become very telling pixels, because they are in color.

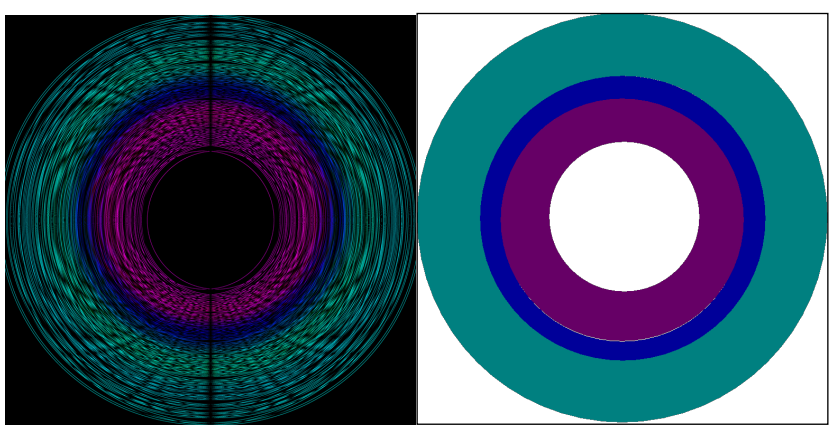

Fig. 18 The fingerprint of Earth 2.0 suggested by a direct observation of an exoplanetary system

A pale blue dot is **blue**. Observation in the near-UV/blue where earth shines brightest is a requisite spectral band for finding an Earth analog. The Earth is strong in this reflectance band due to its characteristic atmospheric Rayleigh scattering and the behavior of the phases of water as they absorb stellar black body radiation in the longer wavelengths.[31] Even as solar black body radiation loses flux over shorter wavelengths, the relative brightness of Earth's albedo grows. For all classes of star with irradiance within 300-400 nm, normalized reflectance in near-UV holds a valuable signature for oceans, clouds, snow and ice caps, as well as the protective UV shield caused by upper atmosphere Rayleigh scattering. This was detected by GOMES, a 1990's ESA satellite launched to find ozone but incidentally looking at earth's oceans in the 300 - 400 nm band and taking simultaneous solar spectra.[32] See Figure 19.

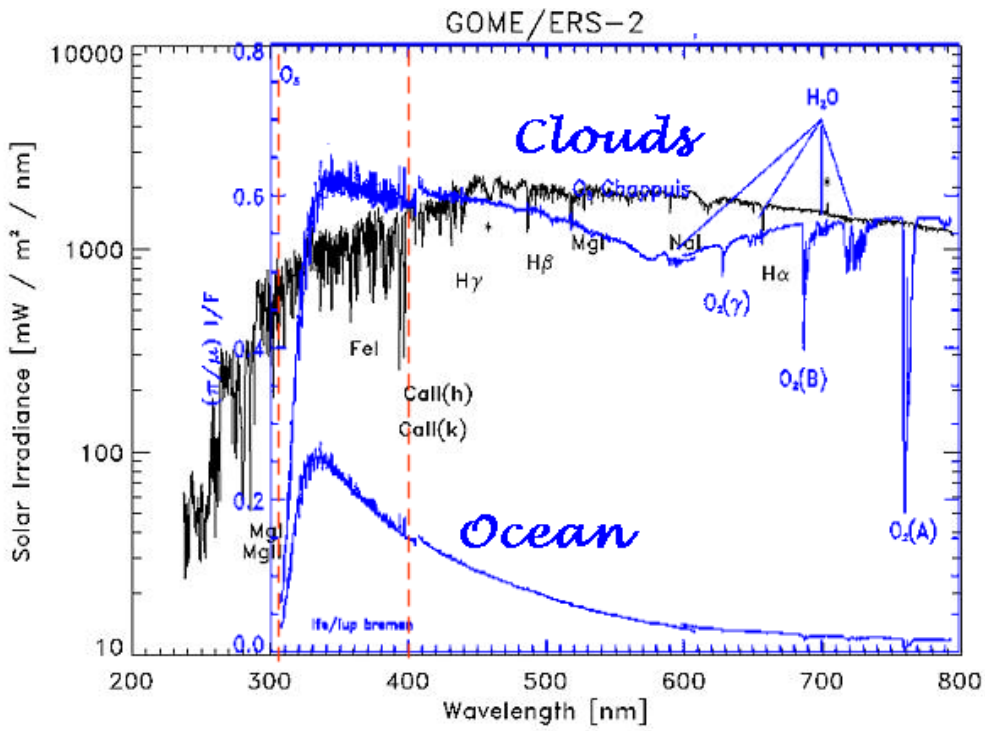

Fig. 19 GOMES solar spectrum (black) super-imposed on earth's water spectra (annotated blue). Band of increasing reflectance of water phases appears in band of decreasing solar irradiance (dashed lines red

Exoplanet hunter telescope concepts shy away from blue and favor the infrared. M-class red dwarfs are being studied, [33] notwithstanding that tidal locking in the habitable zone of these systems precludes an earth twin. [34] The infrared is favored, in part, because star to exoplanet contrast is $1{:}10^{-8}$, whereas relative intensity of parent star to an Earth twin is $1{:}10^{-10}$ in the blue. Infrared telescopes are being readied, particularly from the ground, but they cannot confirm an Earth twin in the blue and near-UV bands. All planets exhibit heat signatures, and it is particularly useful that infrared spectrograms may contain signatures of biological byproducts such as oxygen and methane. That said, Earth twin finder must take spectra in the shorter wavelengths to differentiate exoplanets from each other to say nothing of detecting Earth twin candidates.

4. Basic optical physics of POGs

The behavior of diffraction gratings is quite different than mirrors and lenses, because the grating magnification feature is caused by the interference between periodic waves striking a periodic barrier. The behavior is uniquely characterized by discrete constructive nodes, the diffraction orders n, integer multiples. Reflection and refraction do not exhibit this characteristic. Prisms show dispersion as gratings do, but notably the magnification feature is inverse to wavelength with shorter wavelengths showing greater magnification. The diffraction equation takes the form;

(8) $$\sin(i) + \sin(r) = n\frac{\lambda}{p}$$

where i is the incident angle as measured from the surface normal
r is the reconstruction or receiving angle as measured from the surface normal
n is the diffraction order (an integer)
λ is the wavelength of the periodic radiation
p is the pitch or period of the grating

4.1 Plane grating objectives

A plane grating, that is, one of uniform pitch, has an anamorphic magnification feature because at angles $r > 45°$ wavelengths λ will separate from each other at greater angles than their incident angles i. As r approches 90° angles of r approach "grazing exodus" where spacing between received wavelengths extend toward the infinite. This is not fantastic, because for infinite magnification, the plane grating would need to be of infinite length. Yet there is optical leverage similar to a mechanical lever, exampled in Figure 20.

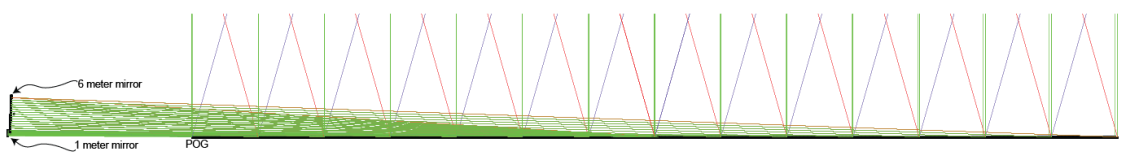

Fig. 20 Rays from sky diffracting at grazing exodus from a POG to secondary mirrors on the left.

In a practical embodiment of a plane grating telescope, a secondary focusing mirror forms the image of the sky on a slit. The anamorphic magnification is the ratio of the length of the grating divided by the diameter of the secondary mirror that focuses the image on the slit. The closer to grazing (the higher the angle of diffraction) the smaller the secondary mirror required and the greater the magnification, Figure 21.

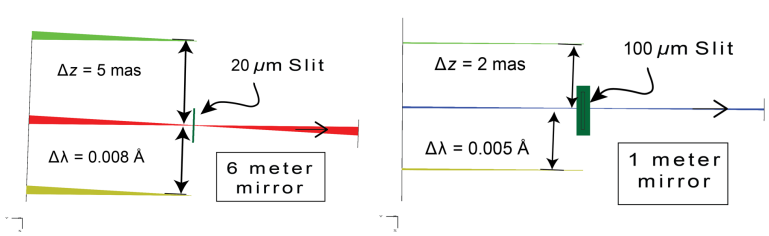

Fig. 21 Δz is the resolved angle on the sky. The 1 m secondary mirror (right) has better than twice the resolution of the 6 m secondary mirror (left), even with a wider spectrometer slit.

This magnification feature becomes useful in astronomy when the wavelengths correlate to resolved lines of sight. The correlation is possible if the secondary is a spectrometer.

4.2 Chirped grating objectives

A secondary focusing mirror is not required if the POG can focus. This is possible if the period of the grating varies across its face. The mathematical model of such a grating is the fringe pattern of a spherical wave at a focal distance with a plane wave, the wavefront from a star. This forms a holographic optical element. The HOE primary objective of the telescope of Figure 12 above is detailed in Figure 22 to show how it focuses light across the visible spectrum for two stars separated by 2°. For any one of those stars, the spectrum focuses sharply over 20 nm, Figure 23.

One advantage of using a focusing HOE as the POG in a telescope is that light is diffracted at an angle that is an approximation of the angle of incidence. Compared to the POG of Figure 22 which collects light at grazing exodus, diffraction efficiency is greatest when light is diffracted at the same angle as incidence (the so-called Littrow angle).

It also must be noted that while a nearly perfect focus can be obtained from an HOE at the wavelength at which the HOE is fabricated, at other wavelengths, the focus blurs.

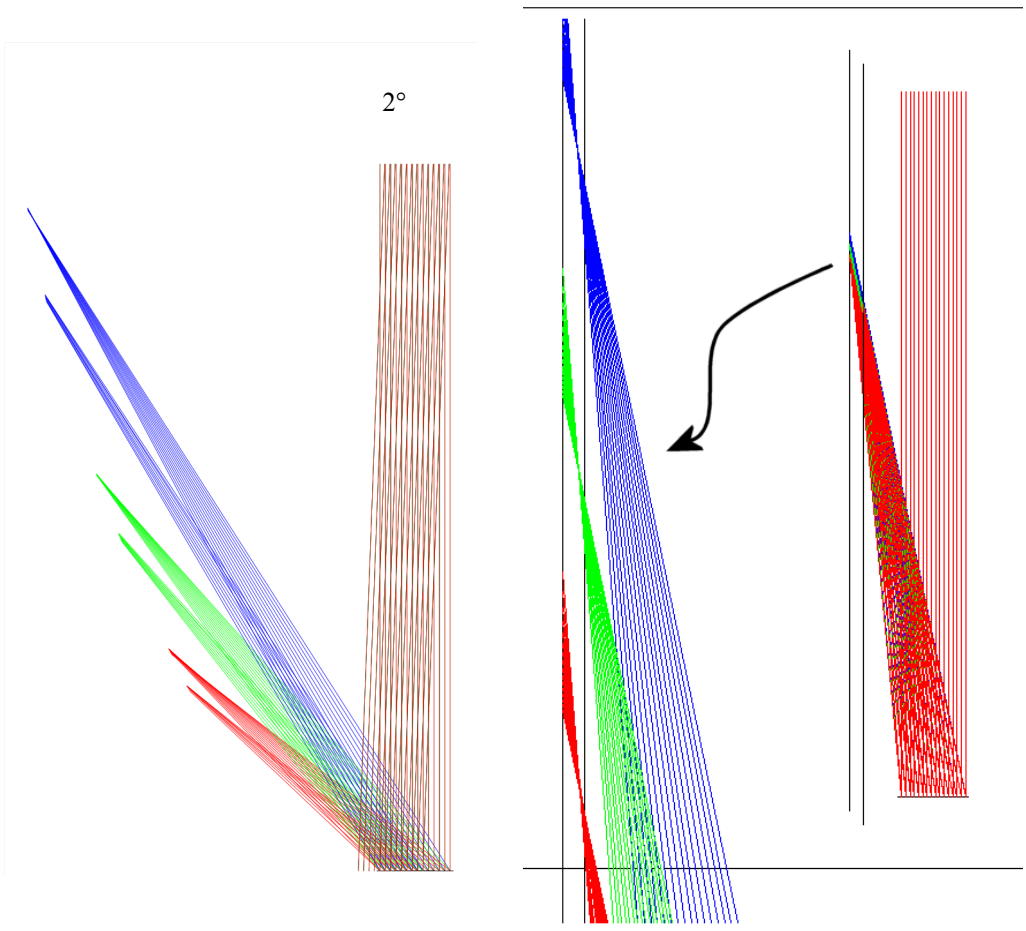

500 and 600 nm

Fig. 23 Sharp focus over 20 nm

4.3 Secondary optics

A POG telescope converts angles on the sky into wavelengths. The resulting variations across the acquired spectrum must then be converted back into the angles on the sky. In other words, the secondary for a POG telescope is a spectrograph that serves two purposes at once, angle and wavelength.

Compare this with a conventional telescope where a fiber may be placed where a star is known to be focused. The fiber in the conventional spectrographic telescope is used as an input to a spectrograph. For each fiber there will be one star and one resulting spectrum. With such installations, the fibers must be moved to a location where there is a star and kept locked in. Sometimes there is not enough room on the focal plane and targets will not be recorded. Also, spectrographic surveys require a prior star map to install fibers.

We are looking for exoplanets that are being segregated by their wavelength, not their position at a specific angle relative to other exoplanets or to their parent star. The concept is quite different from prior telescopes and needs to be understood for its distinction from earlier telescope architectures. In a reflective primary telescope images are taken from angular displacement. Angular resolving power is the critical measure of resolution.

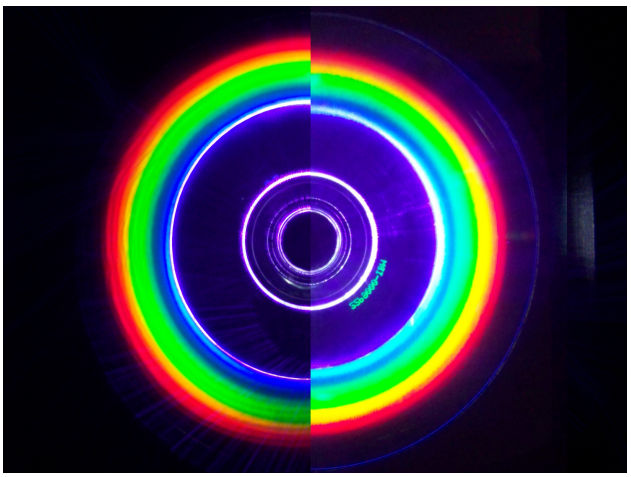

Fig 24 The diameter of a circular spectrogram records the radial velocity of a star by Doppler shift.

Because DUET is a spectrographic telescope, its native record is a spectrogram. With a primary capable of resolving thousandth of an Ångstrom, the secondary disperser can be designed to hold to a resolution sufficient to record the red and blue shifts caused by the motion of the star toward and away from it. In Figure 24 is a demonstration of the process. It compares two observations which changed the diameter of the spectrogram as a consequence of the motion of the observed star. These readings can be interpreted to disclose the presence of exoplanets around the star, their masses and their orbits. This is an indirect method of exoplanet discovery and constitutes one of the two observational methods that led to the designation of the telescope as DUET – Dual Use Exoplanet Telescope.

4.4 Coronagraphy

Coronagraphs tend to be bandwidth limited. Even the starshade, which is external to the telescope using it as an occulter operates within a bounded wavelength band. It falls out from the nature of a POG that many narrow bands are available, each of which can be tuned to block light from the parent star. The many wavelength bands of a POG lend themselves to the development of coronagraphs that exploit narrowed bands.

5. DUET Optics

DUET is a space telescope concept with a Gabor Zone Plate POG configured as a ring or annulus. Our Phase I study looked into modeling DUET optics mathematically, bench testing, identifying targets for observation, and examining data reduction algorithms.

The notion that a space telescope could be configured as an annulus has been explored for a mirror primary.[35] Deployment of TALC, a far infrared 20 m annulus telescope, benefits from stowage of the stacked mirror segments. Once assembled, the demanding figure tolerance of reflection telescopes persists. presenting significant hurdles. The very long wavelengths being observed loosen tolerances to workable levels for TALC.

As we have shown in Section 2.3b, a POG has relaxed figure tolerances. As a gossamer membrane, it has the lowest areal mass of any telescope primary objective. It can be stowed on a mandrel for launch. The aperture across the annulus potentially could reach the 100 m class. The planned observations extend into the near-UV.

5.1 GZP

A Gabor Zone Plate (GZP) has a variable frequency of concentric circular rings similar to a Fresnel lens, a precursor from the nineteenth century when transmission optics were made with glass. The ubiquitous Fresnel lens is a "flat" lens that has concentric rings with lens segments having focal lengths in proportion to diameter. A Fresnel zone plate alters the ratio of line width to work in the diffraction regime where the angle of diffraction is inversely proportional to pitch. A photon sieve is similar but can be micro-machined. Figure 25.[36]

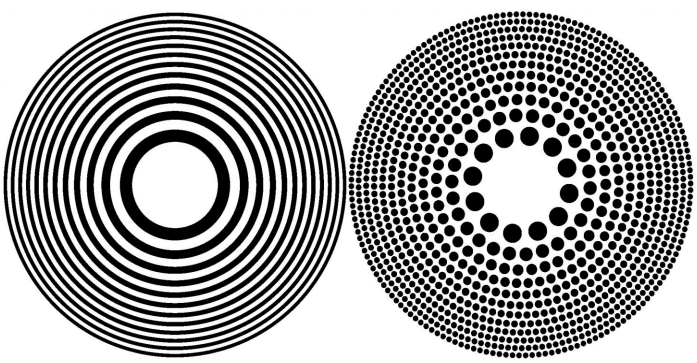

Fig. 25 Fresnel Zone Plate (left) Photon Sieve (right)

A GZP induces a phase delay. The resulting interference focuses a wavefront. Figure 26.

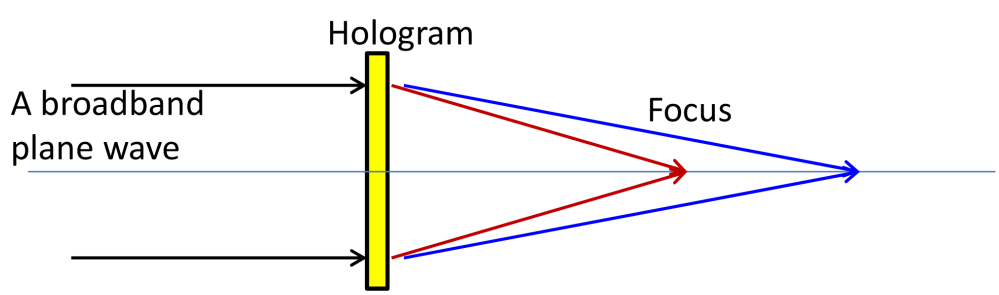

Fig. 26 Behavior of a GZP – A plane wave (star) focuses to a point, wavelength by wavelength

5.1a Bench experiments

A GZP can be fabricated holographically. Generically the hologram is made by the interference of a plane wave and a spherical wave of a single mode laser. We modeled a GZP in Zemax by the plane/spherical wave interference setup. The focal length of the GZP at the recording wavelength is at the point of origin of the spherical wave. Our laboratory's physical version of a GZP was made with two spherical waves, Figure 27.

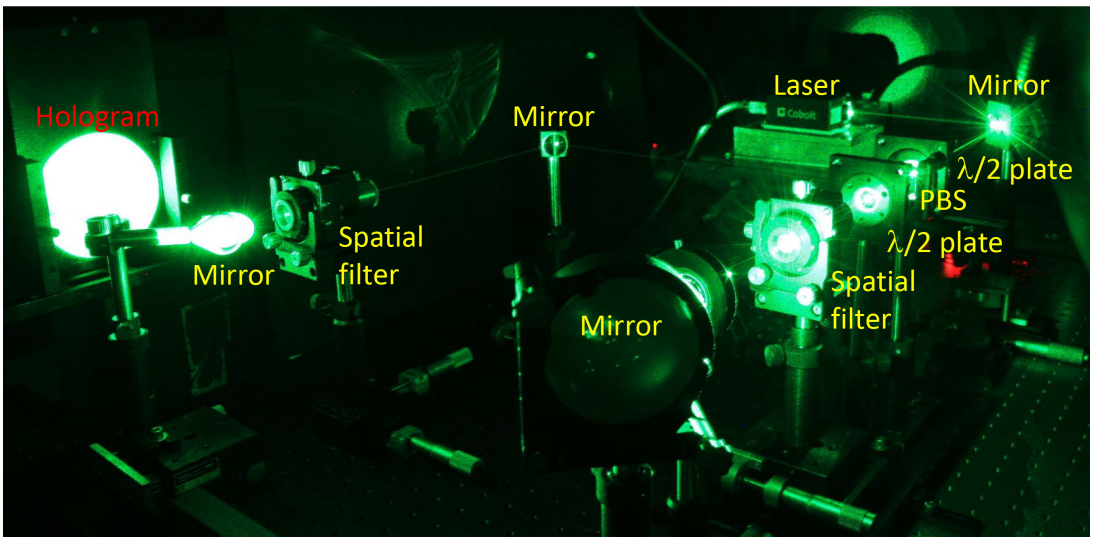

Fig. 27 Laboratory bench for recording our GZP. [PBS: Prism Beam Splitter]

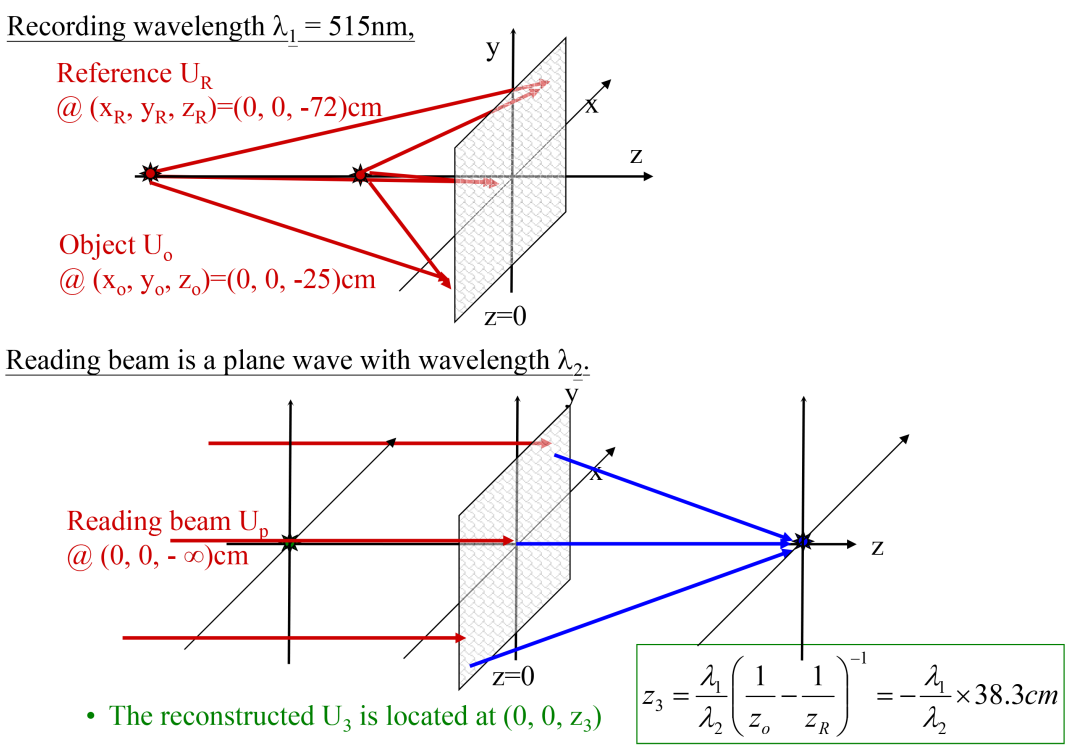

Fig. 28 Analysis for construction and playback of our bench GZP

They share a common axis facing the surface normal of the recording surface, Figure 28.

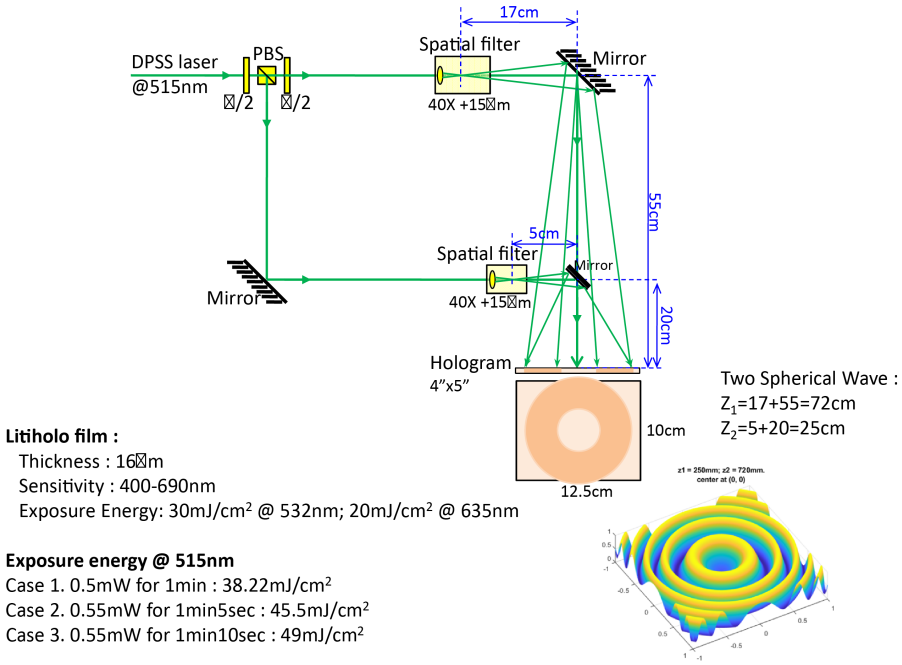

Fig. 29 Schematic for the bench of Figs. 27-28

Bench layout is shown in Figure 29. A series of test exposures led to a 100 x 120 mm GZP plate with an efficiency of 20% at 632.8 nm playback. Predicted pitch variations are illustrated in Figure 30.

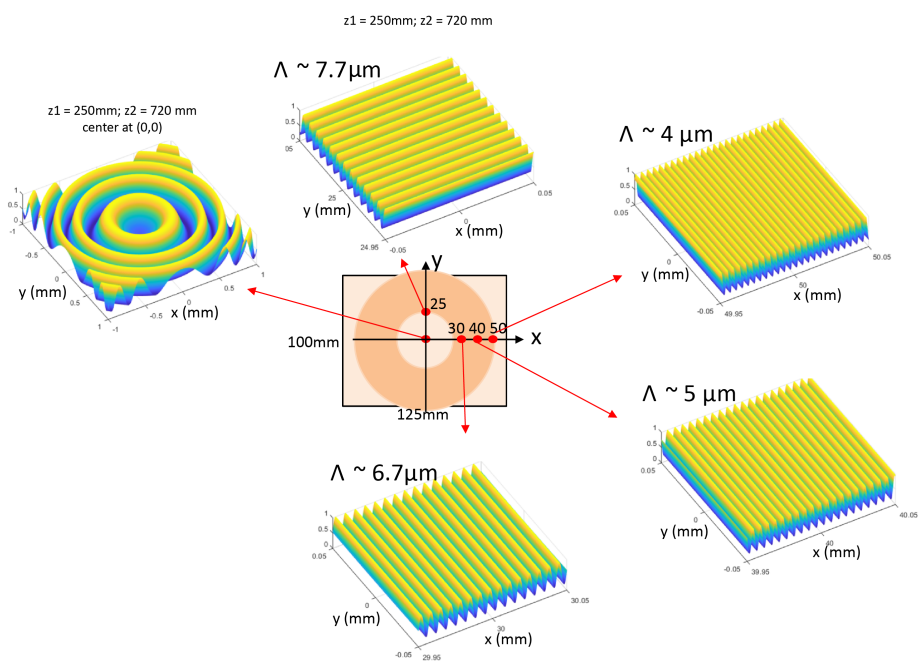

Fig. 30 Interference patterns of two spherical waves (z1 = 72 cm & z2 = 25 cm)

Examined microscopically, the periods Λ conform to prediction, Figure 31.

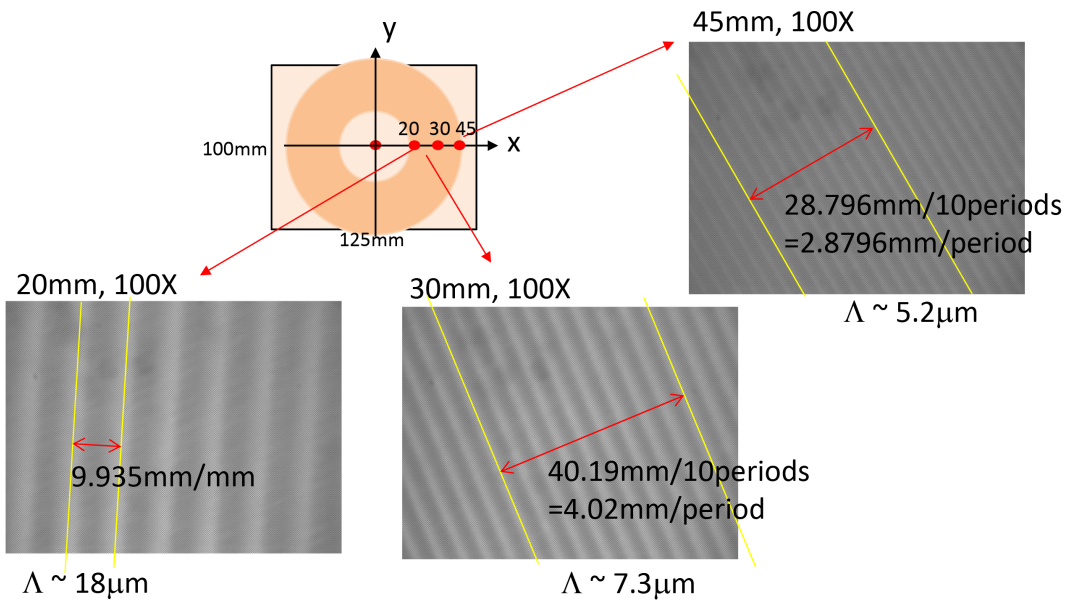

Fig. 31 Microscopic image of GZP periods. Energy of exposure 16.3 mJ/cm2 @ 515 nm

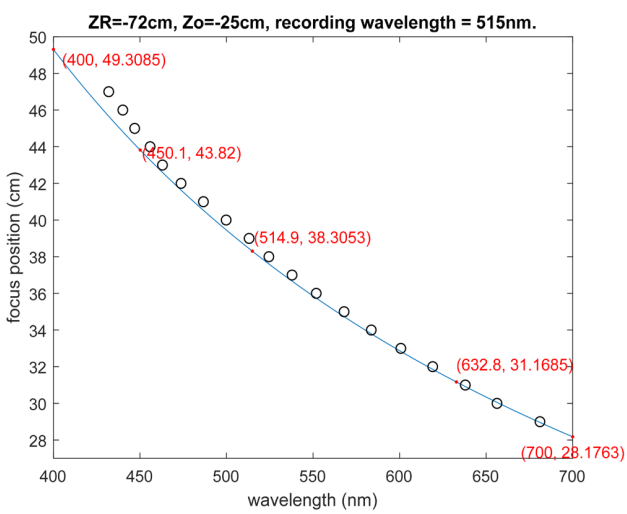

Fig 32 GZP wavelength v. focal length

Predicted focii f of the GZP are graphed in Figure 32 from the equation in sidebar, Figure 28.[37]

$$(9)\quad f = \frac{\lambda_1}{\lambda_2}\left(\frac{1}{z_{obj}} - \frac{1}{z_{ref}}\right)^{-1}$$

where λ_1 = 515 nm
z_{obj} = 250 mm
z_{ref} = 720 mm

The curve is matched against points taken on the bench with this GZP, as indicated by the "o" symbol marking each reading.

The bench used a fiber fed spectrometer which captured the wavelengths at increments along the central spine where the GZP focuses. Given the considerable diameter of the fiber tip, 400 µm each band is distributed into a Gaussian function from which a centroid can be taken.

The bench and a spectrum taken from a blue LED with a yellow stimulated phosphor is shown in Figure 33.

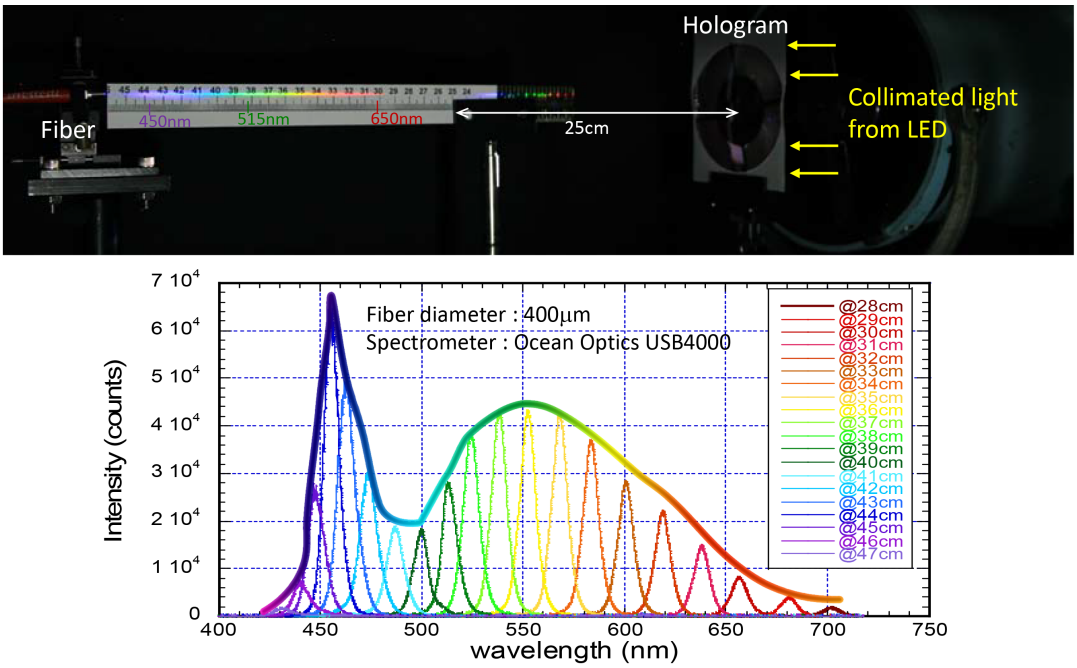

Fig. 33 GZP spectral distribution from a "white" LED

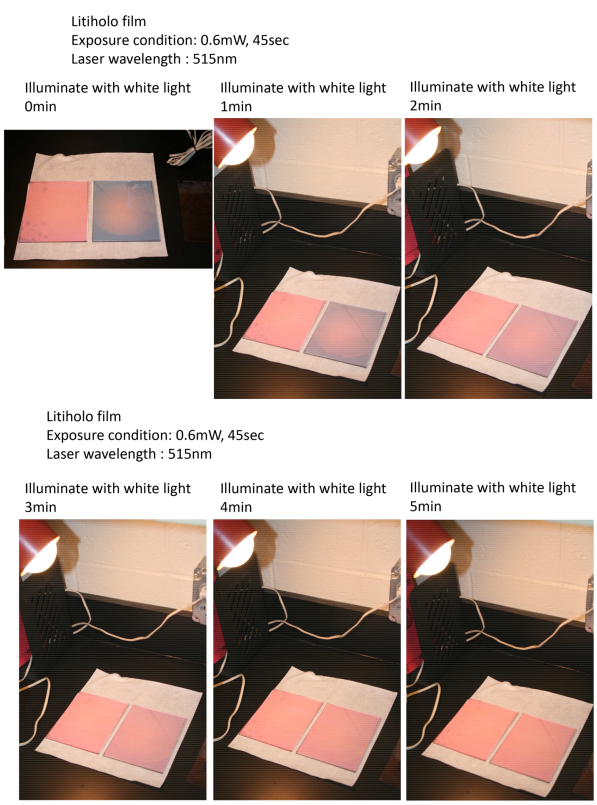

Fig. 34 Dry development of Litiholo film

The GZP was recorded on Litiholo polymer holographic film which qualifies as a gossamer membrane. It is 16 µm thick. It is supported for exposure by a 1.8 mm glass plate and strengthened on the other side by a 50 µm PMMA acrylic plastic transparent film. After exposure, Liti polymer is dry developed in broadband light and stabilizes in a few minutes. A development sequence is shown in Figure 34. A reference developed sheet is on the left. The GZP can be seen by the partial development on the right which is partially blue. After five minutes both the fresh exposure and the reference are the same color. The GZP, a phase hologram, has been recorded, developed and remains stable in room light.

Using a compact disc with a fixed pitch of 1.7 µm in a near perfect

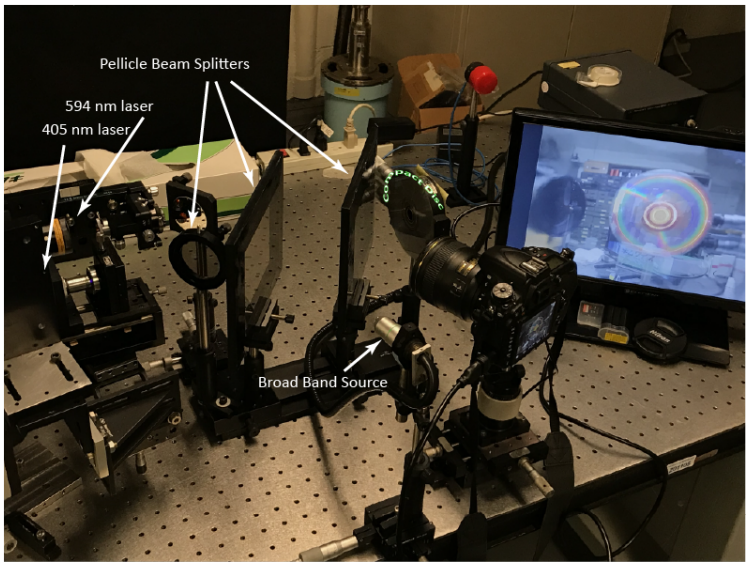

Fig. 35 Compact Disc simulation of GZP annulus dispersion

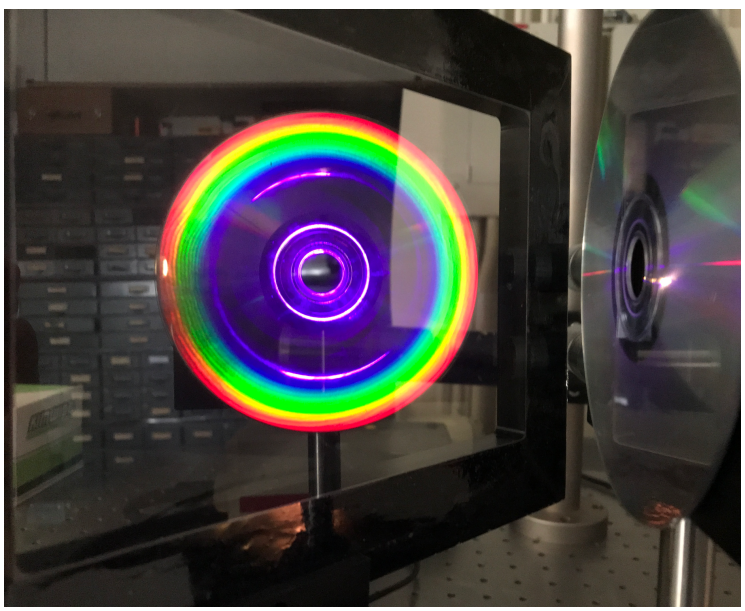

Fig. 36 CD seen on-axis through large pellicle beam splitter

When to 405 nm laser is geometrically on-axis it forms a circle that matches the broad band source, Figure 37. These images have a central violet circles that are caused by the refraction of the totally internally reflected light exiting the plane of the CD near the hub which has a slight prismatic refraction structure molded into the disc. We found this convenient as a geometric reference, but it does not exist in either a GZP or circular plane grating.

circle (the form factor is, in fact, a spiral), we simulated the dispersion of a GZP.

Examples of the experiments are shown in Figures 35-37. The bench with the CD, two lasers each with a 25 µm pinhole spatial filter, an incandescent broad beam source, pellicle beam splitters, and a camera are shown in Figure 35. A shared image of the CD and its on-axis image as seen through a beam splitter, Figure 36. Note that the 405 nm laser is slightly off-axis in the setup and produces arc segments rather than a matched circle. The paraxial geometry is extremely sensitive, a phenomenon that can be exploited in coronagraphy as detailed in Section 5.3 and in competing source removal, Section 5.3c.

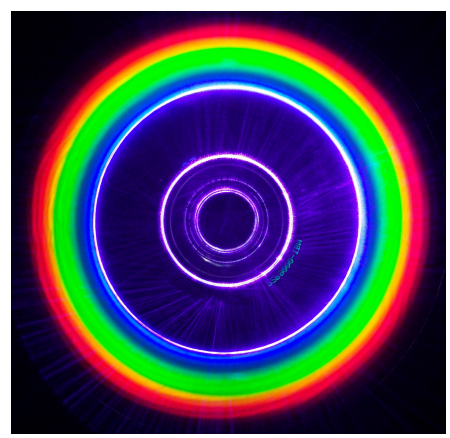

Fig. 37 Violet laser on-axis

5.1b Annulus

The concept for DUET is a GZP POG with a secondary spectrograph. A schematic is shown in Figure 38. The circular colors are not a realistic portrayal, since an off-axis view angle on a GZP produces "spokes" of color, as one would see on a compact disc or DVD. The only way to obtain spectral rings is to view the GZP directly on-axis. That said, the secondary Receiver is portrayed as it would appear to the eye. A GZP focuses light inversely proportional to wavelength with red bending the most. However, the focus would be along a central axis.

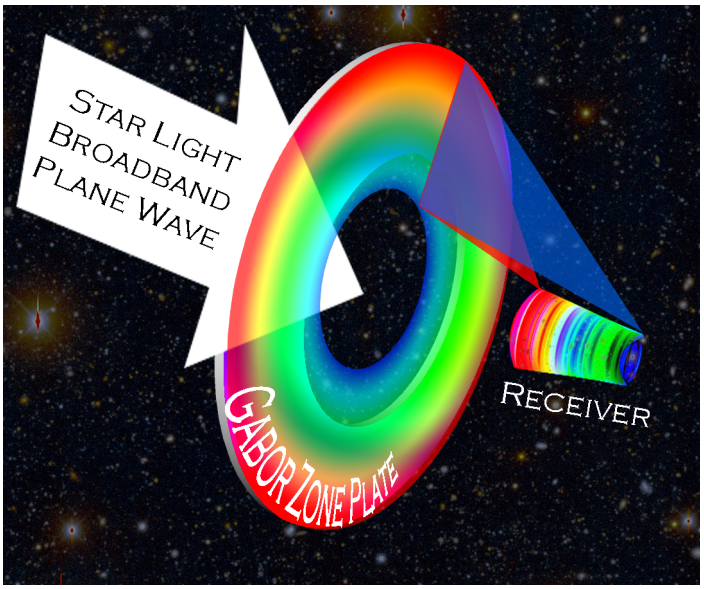

Fig. 38 DUET schematic as submitted for NIAC Phase I

We took a liberty in the schematic of Figure 38 of showing the visible spectrum, when our planned observations would include the near-UV. Another rendering which perhaps lacks schematic clarity, Figure 39, attempts to illustrate the proposed band that interests us in the search for an Earth analog as described in Sections 2.1 and 3.3 above. The support structure that would hold this telescope together is detailed below in Section 6.2.

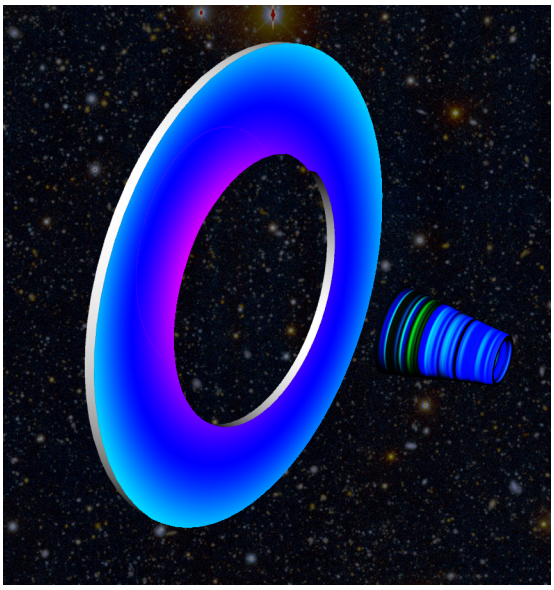

Fig. 39 Rendering in the near-UV band

When studying chirped POGs, illustrated in Section 4.2, we learned that the focus was tuned to the wavelength that creates the GZP. In our Zemax model of DUET we selected 405 nm for as the central wavelength, both as a reasonable pivot around the differential measurements of the target objects in shorter visible and near-UV and also to accommodate our laboratory instruments which includes a single mode 405 nm laser for the creation of larger GZP's in Phase II.

An annulus with a drum spectrograph allows us to modify the optics so that the ring has an inner and outer diameter equal to the widest optic we can stow for launch while also making the aperture a variable parameter adjusted for optimal performance. At the moment, our models assume a 10 m ring inside a 50 m aperture.

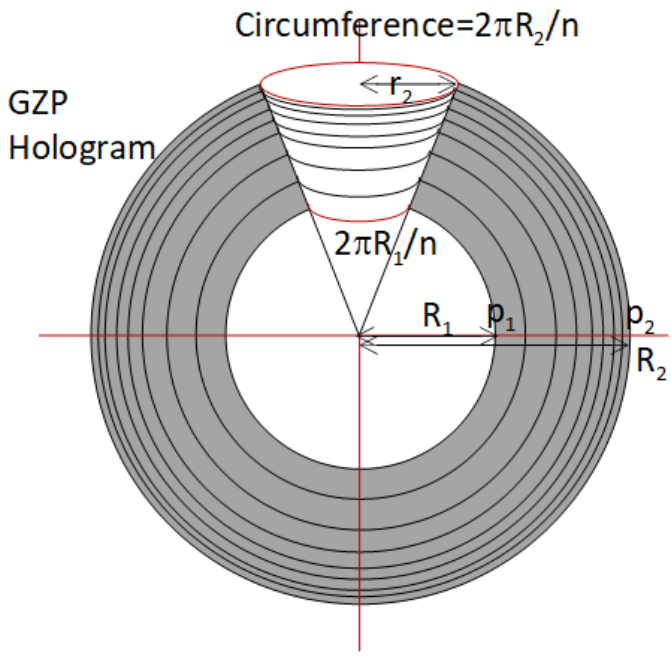

Fig. 40 Drum embossing a GZP

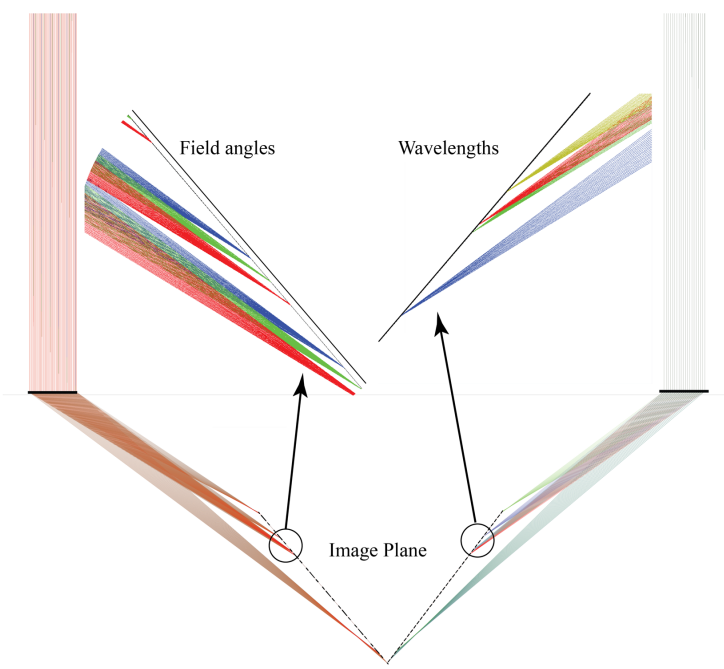

Fig. 41 Notional GZP focuses onto a conical image plane shown in cross-section. Spatial separation of exoplanets from parent star is indicated by field angle (insert left) covering the f-o-v of 36 arseec. Wavelengths (insert right) are centered on 405 nm and span 40 nm.

While it is possible to make a GZP by direct exposure on a holographic plate, as we did in Phase I, the pure symmetry of the HOE affords us a means to create an embossing master that extends the diameter of the GZP to the active region of a hologram created on a cone, as illustrated in Figure 40. Print masters are routinely made on drums to extend the length of a matrix of replicas in keeping with the printing press paradigm.[38] Our approach is similar, although not known to us in the literature for the creation of large optical elements on thin flexible substrates. Creation and printing from such a surface relief holographic master is a proprietary project planned for our NIAC Phase II.

When an annulus is constructed from a ribbon formed by the embossing method of Figure 40, the focus can also be annular depending on the choices of the inner and outer circumference, allowing construction of a secondary receiver as conceptualized in Figures 38-39 which is a truncated cone that houses a spectrograph.

As a design choice for the DUET space telescope, we elect to fabricate this portion of the secondary on the ground. It holds the spectrograph and coronagraphs. We detail its optics in Section 5.2 – 5.3 below. A Zemax model of the GZP with annular focus is

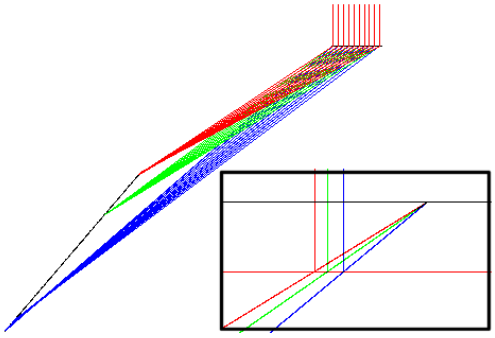

Fig 42 Chromatic dispersion detail of Fig. 41 covering 40 nm over 36 arcsec. Insert compares incident angle with dispersion .

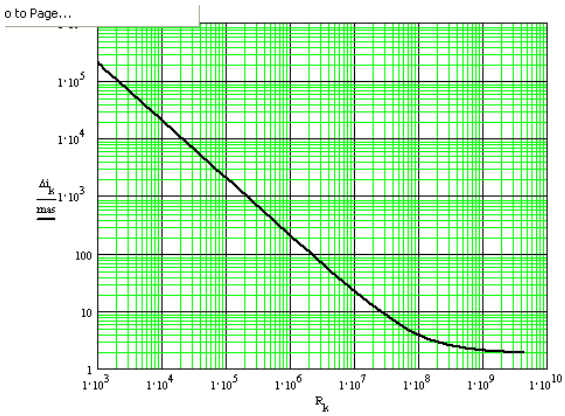

Fig. 43 Limit on resolving power of 10 m GZP

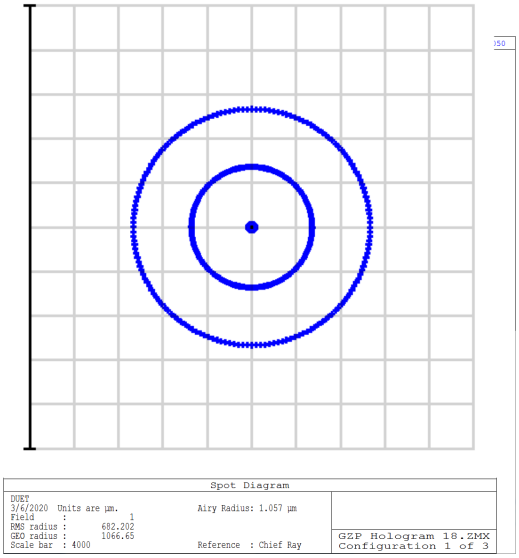

Fig. 44 GZP Spot Diagram

shown in Figure 41. In Figure 42, the right hand detail of is magnified to show the dispersion of the GZP over the wavelength range.

The resolving power is proportional to the considerable width of the GZP ring. The DUET concept has up to a 10 m ribbon to fit on a stowed mandrel under the launch vehicle faring. The ConOps are in Section 6. If the GZP has a 10 m considerable width, the theoretical resolving power as per Eq. (1) is shown in the graph of Figure 43 to approach but not quite reach 1 mas. As a practical matter it may be on the order of 10 mas.

The annulus itself may span 100 m which would push the resolving power past 1 mas, but in order for the phase to remain locked over the considerable diameter, the 10 m gossamer membrane would have to be stable across opposed sides to nanometer precision. While not impossible as a long term goal for a telescope of this type, we deem it an unrealistic specification for the earliest iterations of DUET or its immediate derivatives. Our goal is to find and take spectra of exoplanets. Working within a 10 mas resolving power should suffice.

Zemax predicts that an annulus will exhibit secondary and tertiary rings around the central point of focus, Figure 44. These aberrations, if they persist in future iterations must be addressed. In part, the arc segment of the GZP that will be used represents a few degrees of arc over entire ring, simplifying the problem, but contamination of adjacent pixels must be avoided to retain the full spectral resolution of the primary. In the example, the outer ring is a millimeter off the center. That falls within a window that can be collected completely by secondary optics if we manufacture the secondary from discrete mm scale photonic chips

5.2 Secondary

Physical fabrication of secondary spectrometer optics were beyond the scope of Phase I, but we did model a spectrograph in Zemax using the variable pitch hologram function supported by this software. Instead of using lenses to focus the image of each spectral element, HOEs were modeled for narrowly selected wavelength bands. Spectra are redirected toward a sensor plane in the secondary, Figure 45. The change in angle is well suited to the physical optics of diffraction. DUET has no lenses or mirrors.

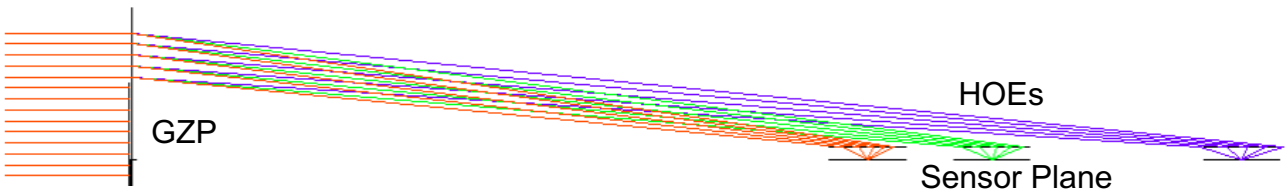

Fig. 45 Zemax model of chirped HOEs that redirect the spectrum down to focus on to a sensor plane

The exemplary spectral bands of Figure 45 are modeled for three wavelengths. In Phase II we will study two methods to widen the spectral bands and optimize efficiency. The analog hologram of Figure 46(a) produces a 1-D chirped HOE that focuses in a band centered on 515 nm. Examples of this disperser can be made experimentally using the same holographic bench we used for the GZP of Figures 27-29.

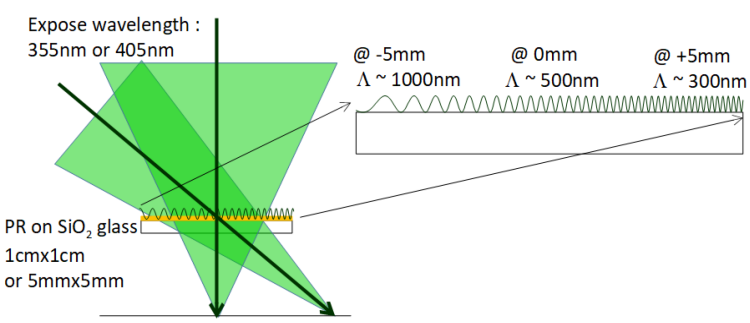

Fig. 46(a) Instantaneous analog exposure method for HOE

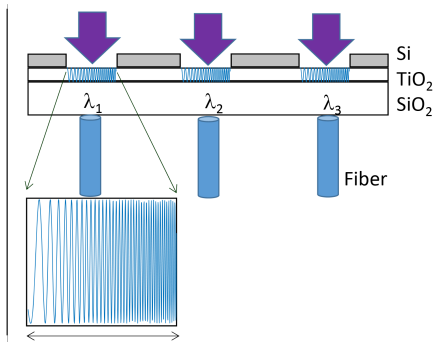

Fig. 46(b) Lithographic Photonic chip

The alternative lithographic method of Figure 46(b) produces a 1-D e-beam chirped photonic chip coupled to optical fibers. In Section 5.3d we note that BLOC is a fiber-fed coronagraph, and a lithographic photonic chip lends itself to the lossless fiber coupling desired. Our proposed grant budget allows a one layer chip. Follow-on support will lead to multiple layers that increase efficiency. The nature of the secondary allows for centimeter scale chips, each tuned to a specific wavelength band. Going forward, established chip fabrication regime with wafer-scale substrates that are diced into segments will be compatible with development of a robust solid state secondary that can be launched from the ground already assembled.

The ConOps of Section 6.2 presupposes a secondary spectrometer in a cylindrical or truncated conical form factor that carries the assembled dispersive elements suggested in Figure 46.

5.3 Coronagraphy

Angular and spectral resolution hurdles for direct observation of exoplanets are daunting, but without a coronagraphic method to overcome the billion to one glare of the parent star, a large POG would collect overwhelming starlight that would block out the faint light from its planetary system.

5.3a ADI – Angular Differential Imaging

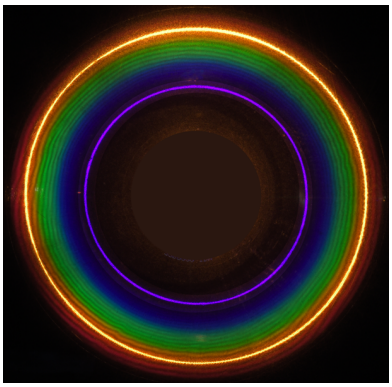

Fig. 47 "Exoplanetary system"

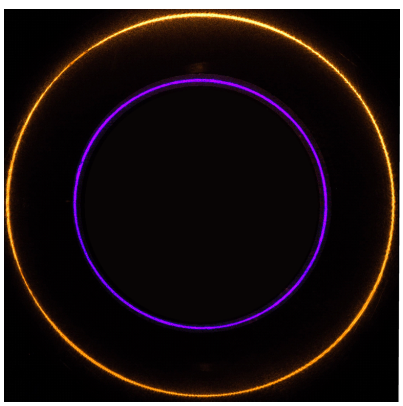

Fig. 48 Two acquired λ's

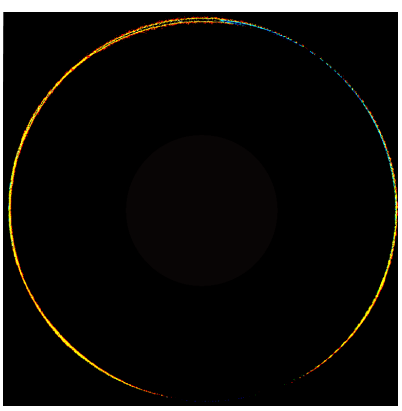

Fig.49 Subtract 405 nm line of "star" leaves 594 nm "exoplanet"

The circular pattern of a DUET spectrogram offers a benefit when pursuing Angular Differential Imaging (ADI) [39] as a means to isolate exoplanets from the glare of their parent star. We did not invent ADI, but it is difficult to practice with mirror telescopy, in part, because the star imaged with a mirror is a point source distorted by asymmetrical artifacts endemic to paraxial mirror telescopes resolving to 10 mas.

In Figure 48 we produced a circular spectrogram similar to what would be obtained by the DUET secondary. Figure 35 shows the bench setup used for our experiment. Beam splitters combine a broadband source with lasers at 405 nm and 594 nm. (The refractive center hub seen in Figure 37 is masked out in Figures 47-49 for clarity.)

Our experiment was purely geometric. We did not establish a 10^9 difference in illumination levels between any of the sources. If the images were recorded to 16 bits, the ADI procedure we are investigating would require better than 15,600 iterations to knock out the star. The iterative data reduction amounts to image processing 10 minutes of movie film frame by frame and is a different problem. The problem is the precision of the optics. Our experiment was to place a 594 nm source slightly off the central axis at a distance we would expect to find the Habitable Zone of a G-class star at 10 pc. The magnification of the circular grating is ~2000 times the diameter of the two point sources used in Figure 48. The experiment was limited to two wavelength bands, In Figures 47-49, our 1.7 μm pitch grating disperses a 25 μm pinhole at λ= 405 nm into a geometric circle 4 cm in diameter. This simulated star line was superimposed over itself and subtracted out. An "exoplanet," also a 25 μm pinhole but at λ = 594 nm offset as it would appear with a 10 m GZP (140 mas off-axis), remains visible after the subtraction, Figure 49.

5.3b Absorption Line Subtraction

In the spectral band that most interest us, 300 – 500 nm, absorption lines are strong. Using the Sun as an example the peak to valley excursions approach 1000:1, Figure 50.

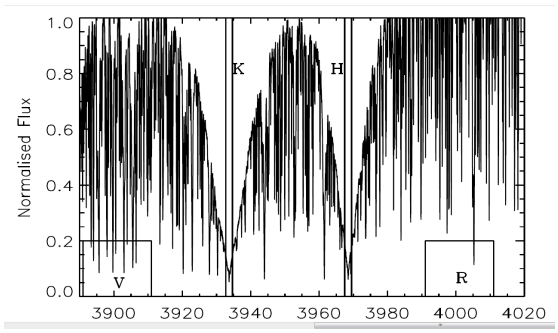

Fig. 50 Near-UV absorption lines of G-star

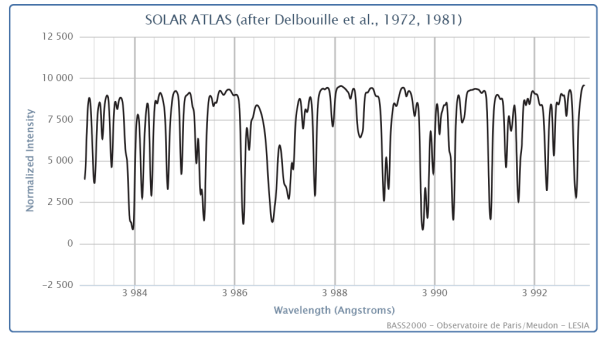

Detail showing Sun in near -UV over narrow band

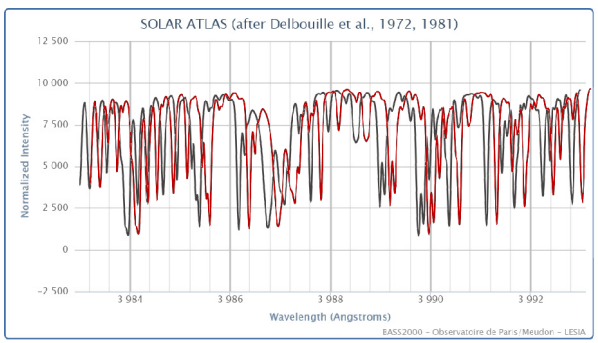

Fig. 51 Simulated shift of absorption lines

As exampled in the ADI process described in Section 5.3a, spectral lines of exoplanets do not line up with their parent stars. Where the offset corresponds to an exoplanet peak superimposed over a star trough, as can be seen in the superimposed lines of Figure 51, the combination slightly decreases the intensity of the star by an order of magnitude to three orders of magnitude.

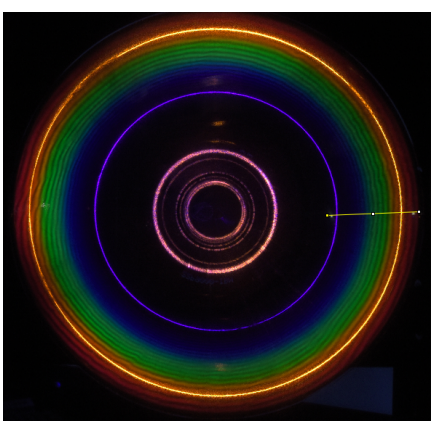

Fig. 52 Profiles taken at straight line.

In the simulated exoplanetary system of Figure 52, we looked at the shift of absorption lines taken from profile plots of Figure 53. On the right, a peak matches a trough. Violet and yellow laser lines are used as static fiducials.

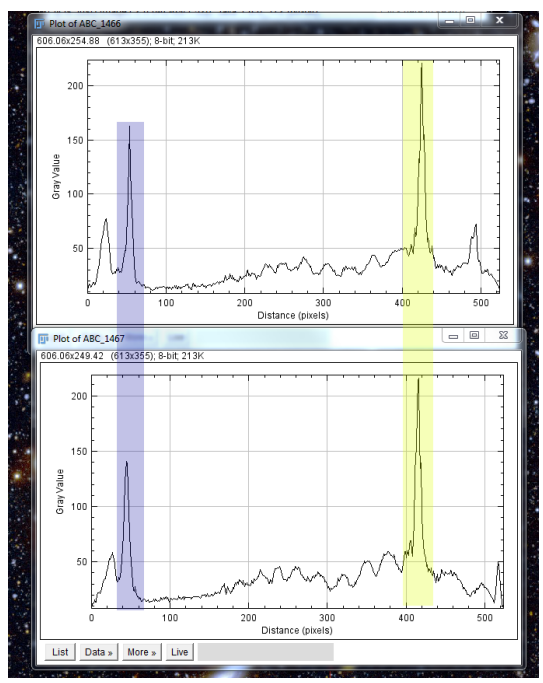

Fig. 53 Shift of “absorption” lines

5.3c Off-axis spokes

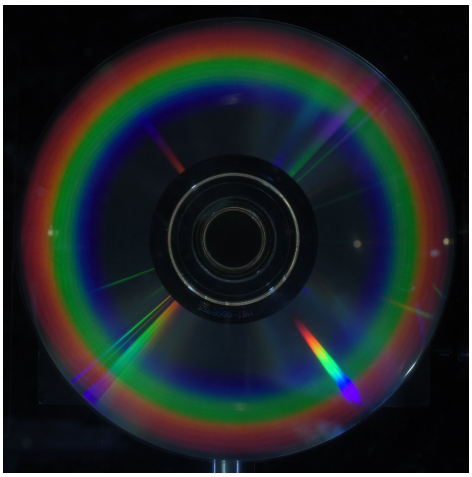

Fig. 54 Off-axis sources leave streaks

DUET observes one star at a time. Other stars will compete with the spectrum of the target star. The commonplace image of a circular CD diffraction grating simulates this interference. Off-axis sources produce “spokes” of color, Figure 54. Most off-axis sources are masked by the inlet tube light shield of Figure 71. Where they do occur, unwanted spectra do not match the wavelengths of the target star, because they arrive off-axis and diffract at different angles for any particular wavelength. An example of a mismatch in wavelength is illustrated by Figure 55. It can be filtered in the secondary where narrow wavelength bands are established by the secondary optics described in Section 5.2.

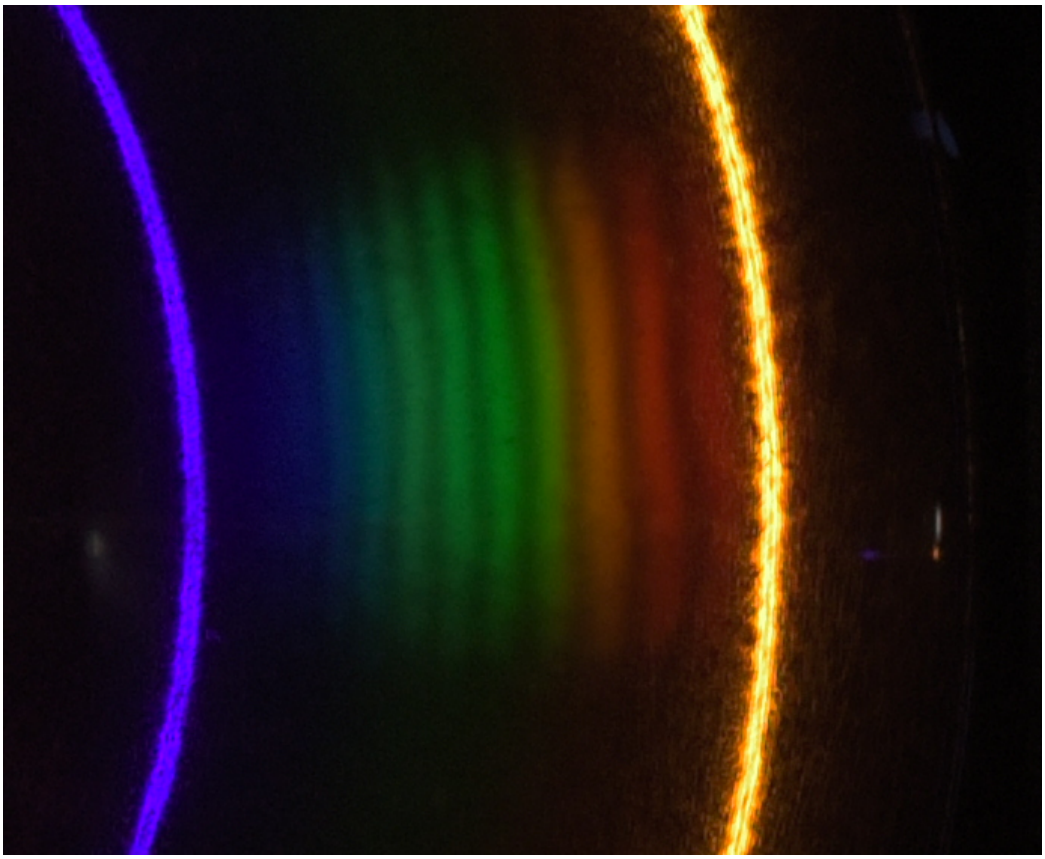

Fig. 55 Simulated off-axis star spectrum relative to on-axis fiducials: violet and yellow Arrow points to yellow in the off-axis spectrum. It can be filtered out of an on-axis spectrum.

5.3d BLOC – Bifurcated Light Optical Coronagraph

Reaching back nearly 20 years NASA has been studying space telescopy for exoplanet discovery. The Terrestrial Planet Finder [40] was conceptualized in two embodiments, one an interferometric telescope and the other housing a coronagraph, TPF-I[41] and TPF-C [42] respectively. Both aspired for more than two octaves of bandwidth, but the wider the bandwidth, the more compromised the performance. A lesson learned from TPF is that coronagraphs generally perform more effectively over narrow bands.

A spectrographic telescope like DUET is ideally suited to attenuate a parent star's flux wavelength-by-wavelength, sharpening the cut-off between the star and coronoagraph's inner working angle, so we invented BLOC, the Bifurcated Light Optical Coronagraph.[43]

In Section 2.2 Figure 11 above, we illustrate a POG, a flat surface with a plurality of re-radiators. The native output of a diffraction primary permits a "divide and conquer" wavelength by wavelength approach to the problem of parent star nulling.

To preserve phase of incident periodic wave radiation, astral interferometric telescopes such as TPF-I assume equal path lengths for all rays from the source star to the image plane. This would seemingly rule out interferometry from flat diffraction primaries such as a POG type of telescope, because path lengths are intrinsically unequal Figure 56.

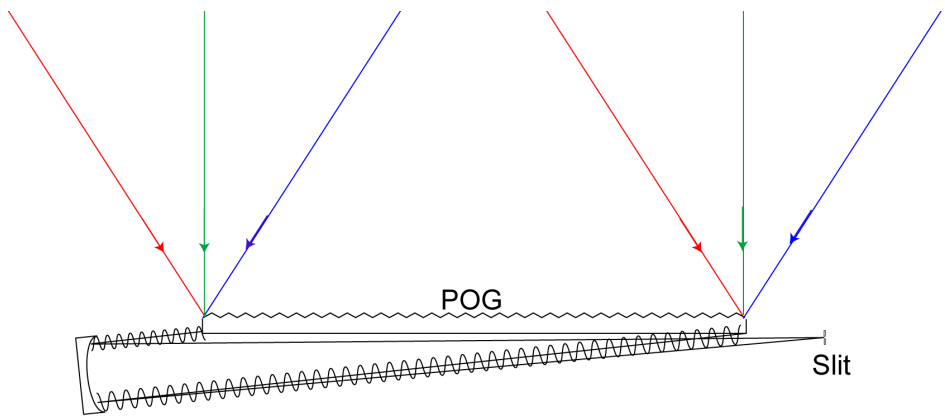

Fig. 56. Path lengths from POG to secondary mirror are unequal. Interferometry is impossible.

Other than a central column perpendicular to the grating plane (green in Figure 56), the wave trains arriving at the POG from angles away from the grating plane normal are out of phase with each other. Inside the telescope, the path lengths are also unequal as they travel from the POG to the secondary parabolic mirror. However, waves from the mirror to the slit can preserve phase. A complete spectrum is illustrated in Figure 57.

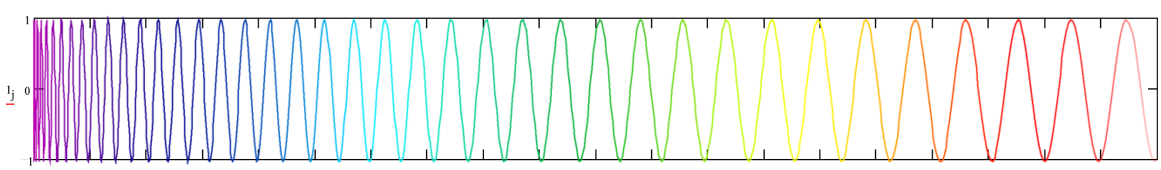

Fig. 57. Full bandwidth output of the POG and secondary parabolic mirror at the spectrograph slit

The wavelengths focused on the slit are caused by an interference phenomenon. There is an integral multiple wave delay from groove to groove of the POG, a phenomenon which results in the whole number integer diffraction orders in Eq. (8). For a fixed angle of reconstruction of the wavefront, there are specific wavelengths that correspond to specific angles of incidence upon the grating. A POG telescope is not an interferometer, *per se*, but the off-axis design of the POG permits a pair of symmetrically opposed secondary mirrors, Figure 13. Symmetry allows the same POG to be used twice. This has several advantages over a single mirror. With respect to astral interferometry, the two path lengths can be equalized in length before the two mirrors are combined, Figure 58.

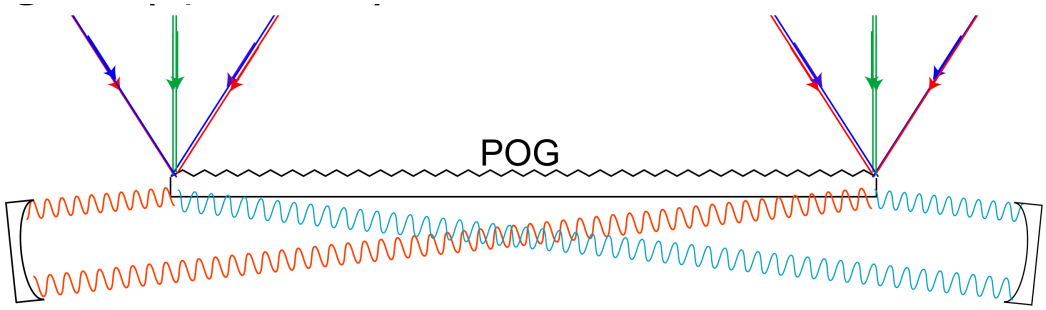

Fig. 58. A second mirror placed in an equal and opposite position on the same POG can match the output of the first mirror

The outputs of the two mirrors can now be combined as they are in a dual mirror astral interferometer. A Zemax model of the resulting embodiment is shown in Figure 59.

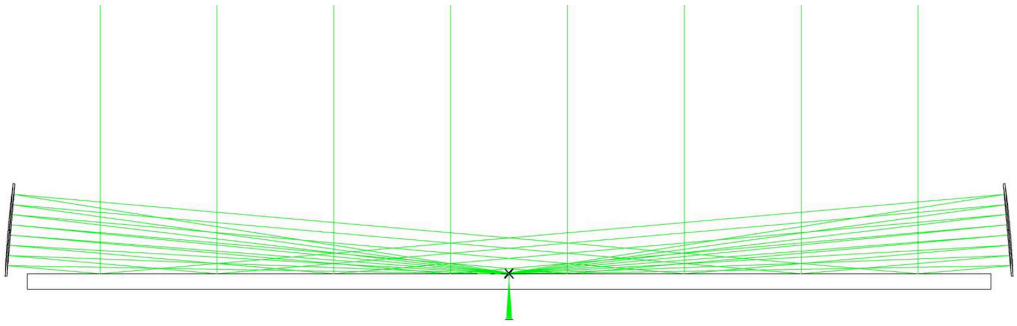

Fig. 59. Zemax model of symmetrical mirrors. This POG is in a reflection mode. Incident rays are perpendicular to the grating plane. The pair of *focii* are combined

If two wave .trains that are equal and opposite they can be superimposed, Figure 60.

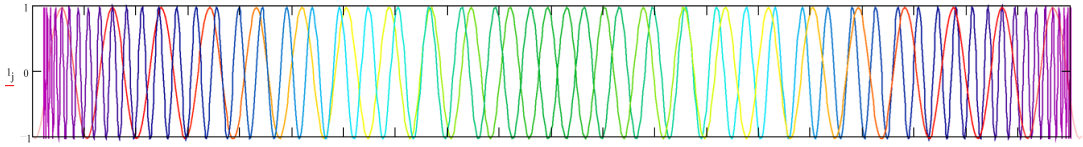

Fig. 60. Symmetrical superimposition of two wave trains that are equal and opposite

As shown in Figure 61 there is a narrow region in the center where waves lengths are identical and can interfere to create an interferometric null. We have modeled this interferometer in Zemax using its Interferogram function.

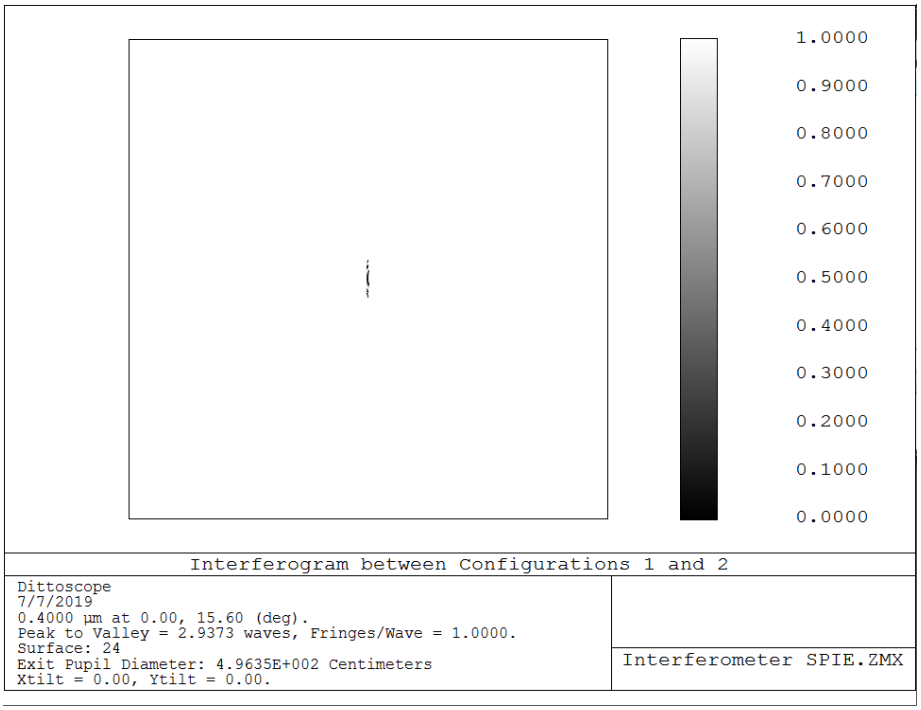

Fig. 61. Symmetrical superimposition of two wave trains - equal and opposite.

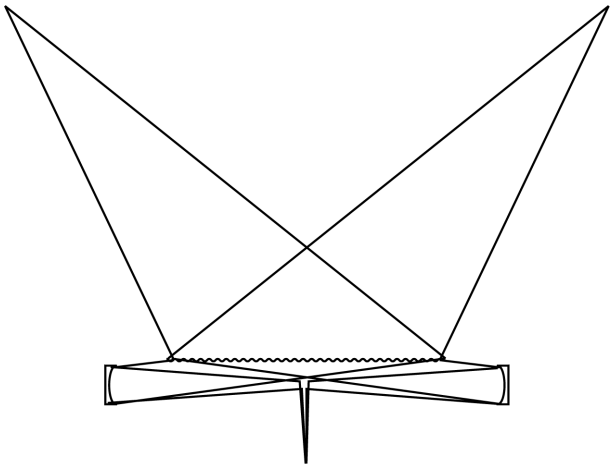

Fig. 62 Interferometer in the near-field (transmission POG)

Admittedly, the null is tiny, but that corresponds to the size of the star that will be blocked by coronagraphy. The remainder of the f-o-v is not touched. We have shown that the extinction is a singularity well beyond the calculation power of Zemax which returns values down to 10^{-4}. We were instructed by the software company to program in their ZPL language to overcome the limitations of their software, a Phase II project. We must also replace the model's parabolic mirrors with elliptical mirrors so that the interferometer can be fed with an array of fiber tips in the near-field over all wavelengths. A pair of bi-furcated fibers in the proposed configuration is in Figure 62. These are the distal ends of one bi-furcated fiber from a photonic chip, Section 5.2 Figure 46b, that are being studied for a DUET spectrometer secondary.

6. Materials and Embodiment

POG materials derive from holography. Some are flexible. Relative to mirrors and lenses, they are thin. Their power is related to a consistent frequency of barriers that interfere with incident periodic waves. But nothing is free. Tolerances for flatness error may be orders of magnitude more relaxed than figure tolerances for mirrors, but the periodic spacing must be held to sub-wavelength precision. With contemporary lithographic methods for integrated circuit manufacture, the rule accuracy is now in the 1 nm realm, so when making a segmented spectrometer as the DUET receiver, the photonic chips can hold to the requisite tolerances. However, 10 m POGs are a completely different story. Holding sub-wavelength precision will require extremely stable substrates.

Mirrors routinely are coated with metals that reflect at close to 100% efficiency. Losses from diffractive surfaces, on the other hand, are likely to rob a POG of 80% of the incident radiation. Hold up a transmission hologram, and it may appear to be an ordinary piece of glass. Diffraction only appears off-axis and consists of first- and higher-order light that is invisible except at the diffraction angles. This opens a daunting limitation for astronomical telescopes, because every photon is needed when imaging faint objects. Fortunately, collector scale is expansive relative to mirrors and makes up for losses.

Contrary to myth, people cannot grow wings and fly. Anyone who has held a bird realizes that mass has been reduced. Bones are hollow. Wings are “feather weight.” In a similar fashion, space telescopes must shed mass routinely accommodated by terrestrial telescopes. On the other hand, once outside the pull of gravity, optical surfaces and the framework that supports them can be orders of magnitude less robust than gratings and trusswork on the ground. The challenge is to stow these materials into a lifter and assure that six minutes of acceleration and shaking at launch will not reduce the package to dust.

6.1 Choice of Diffractive Optics

6.1a Phase

The garden variety hologram is a silver halide transmission or reflection type made on float glass covered with a fine grain version of 19th century photographic emulsion. In an age when electronic cameras have replaced nearly two centuries of classical photography, holographers still labor away in darkrooms reminiscent of Mathew Brady’s circa 1865. Unlike amplitude recordings such as photographs or print images, holographers reduce the residue silver with bleach, leaving behind variations in the index of refraction across the face of the plate. This is akin to seeing a white photograph or a clear negative if viewed in room light, but encoded in the emulsion are the wavefronts recorded - now a true three dimensional embodiment of the original scene.

The transition from silver halide for amplitude photography to phase holography was a small step in light sensitive materials. In fact, the original photographic medium, the Daguerreotype [44], a silver plate developed in gaseous mercury, would be an almost ideal material for holography since it is virtually grainless.

The GZP made in our Phase I used a more modern polymer material which can capture phase information inside long chain light sensitive molecules in a plastic. Notably, the Litiholo[45] material we used is incredibly thin, 16 μm, making it suitable for low mass optics. It is so flimsy that manufacturer sandwiches it between a rigid 1.8 mm glass cover

plate and protective 50 μm acrylic sheet.[46] It can easily be peeled from the glass cover plate, and if it was dimensionally stable in the space environment, it would be a candidate for investigation. Our first GZP performed at 20% efficiency at 632.8 nm. Better efficiency is a goal in Phase II.

The most efficient phase materials are a Volume Phase Holographic Grating (VPHG) made in the hydroscopic material, dichromate gelatin, which is typically protected inside sealed glass plates. Widely adopted for astronomical spectrographs [47], VPHG would require special handing in manufacture and packaging, but could be deployed in the vacuum of space without water damage it incurs in Earth's atmosphere. Commercial VPHG efficiencies are routinely reported above 60% for broad bands and can be as high as 90% at specific wavelengths.[48]

In the course of our Phase I we visited Corning Glass to discuss flexible glass substrates that could be used in fabrication of space telescope GZPs. We learned about their development in flexible glass trademarked Willow Glass [49] and were invited to continue our discussions under an NDA. Without compromising proprietary information we learned that Willow® Glass is a two step process, and we will investigate the second step as a means to form an annulus. The optical quality and CTE (10^{-7}/°C) recommend the Willow® Glass for our application, but we do not know if it could survive shaking.

6.1b Surface relief

In the 1880's, Henry Rowland invented a ruling engine for the production of plane gratings, and variations on his means of manufacture remain in use today for the échelle type gratings used in astronomy. Soft metal is deposited on polished glass and then scored by a tool that has a precise blaze in accordance with the central angle of diffraction in the Littrow configuration. Meter scale gratings on thick optical glass substrates have been produced this way. They are inapplicable for space deployment.

Figure 40 of Section 5.1b diagrams a method to replicate large diameter annuli with a mandrel of smaller scale. The method is intended to overcome stitching errors that are endemic to step and repeat methods commonplace with embossed surface relief gratings. The printing master could be made using a variation on the Rowland ruling engine. CNC lathes of high precision could be programmed with the concentric ring pattern. As we have shown in Section 2.3b, the tolerance for surface flatness error is relaxed. A lathe with mil specifications can be programmed to make a workable truncated cone. If the cutting tool leaves a blaze, the mandrel could be scored with the surface relief grooves.

Given a smooth surface, we propose to spin coat the mandrel with Shipley photoresist under clean room conditions and then use a holographic method to produce the master. We do not see any prior art in the literature and at this stage consider our experiment proprietary. The advantage of using any holographic method to make a GZP is that the fringe to fringe error is controlled by the stability of the laser which is intrinsically capable of holding to the sub-wavelength precision, otherwise a hologram cannot be formed. Moreover, the exposure process itself lasts no longer than a few minutes, as compared to scoring grooves with a ruling engine. A sizeable plane grating made by the Rowland engine can take many days.

6.2 ConOps

DUET is planned as an iSAT [50] mission. On the other hand, the receiver that includes the spectrometer, coronagraph and sensors are presupposed to be a clean room on-the-ground assembly, robust enough to survive launch, and sufficiently compact to accompany the structural elements that will support it and the rest of the telescope.

6.2a Launch

A baseline launch vehicle used for ConOps is the SpaceX Falcon Heavy, a currently operational lifter. As a mission conceived for the 2030's this selection sets limitations that may no longer apply in higher-TRL's. If it works for a Falcon Heavy, it will work with come-what-may. The payload under the fairing is shown in Figure 63.

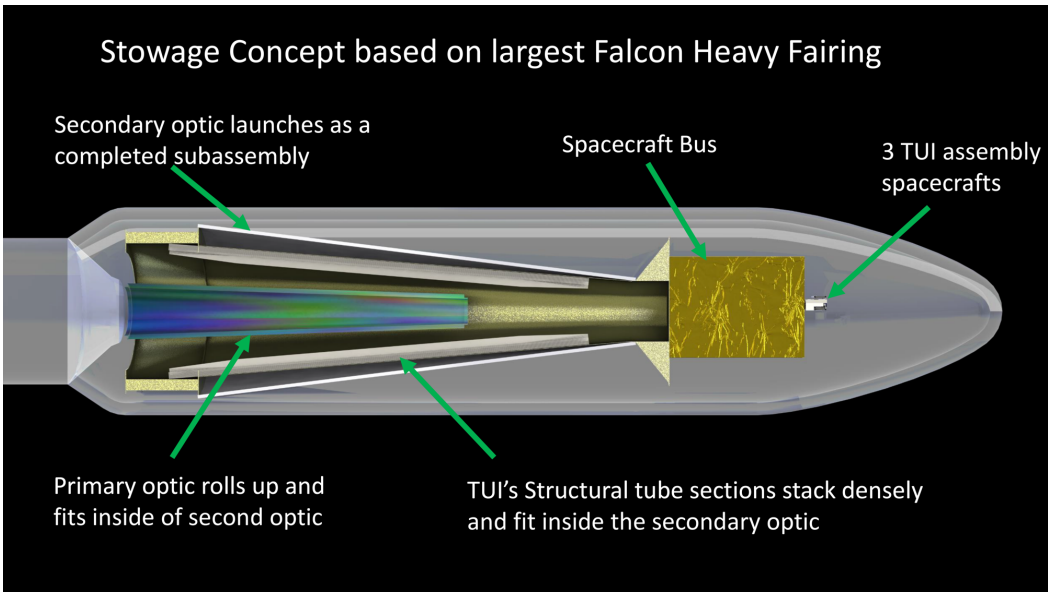

Fig. 63 DUET under the faring of a Space X Falcon Heavy

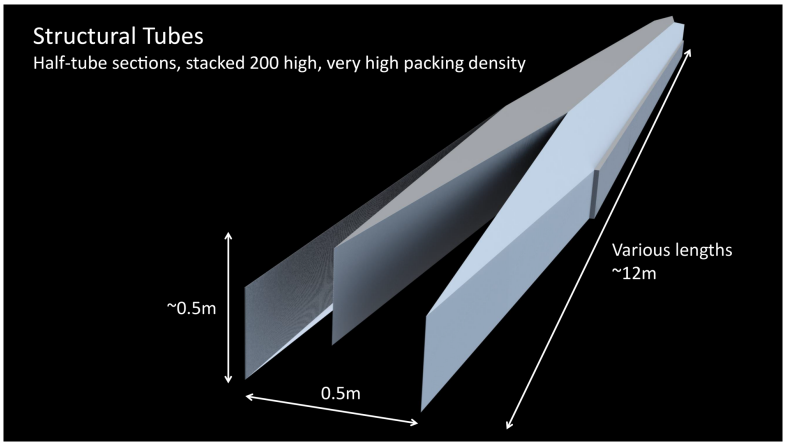

Fig. 64 Under fairing compatible structural tube stack

In the payload are modules, Figure 64, that will be assembled in orbit into the struts for trusses,. Each sub-unit alone is too flimsy to be used as a rigid structure, but once in zero-gravity they will be combined as a set of interlocking units. Their combined strength is geodesic.

6.2b Deployment

In TUI we truss.

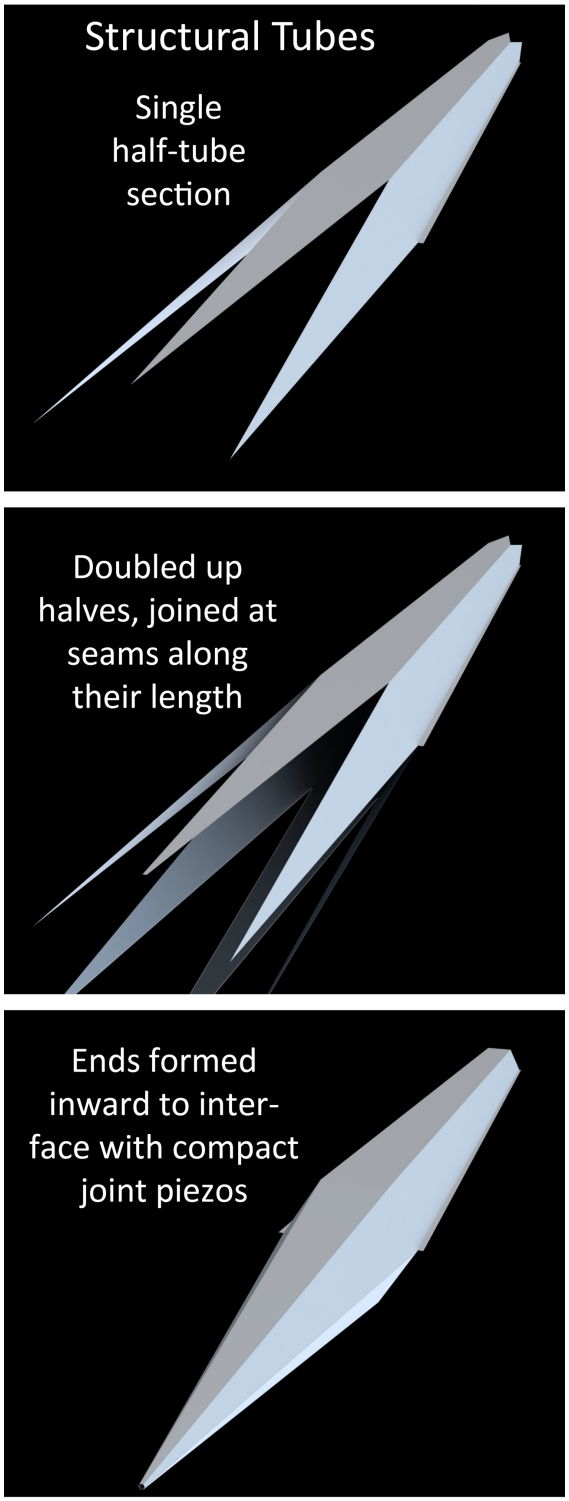

Fig. 65 Assembling a truss structural tube

A lattice of structural tubes are compacted under the faring of a Falcon Heavy launch vehicle. In the TUI concept, struts are assembled from folded half tubes by robots into DUET's truss ribs. Assembly of a single structural tube is shown in Figure 65 in three frames.

Carbon composite material was selected for its low CTE. In addition, the structural dimensions of the truss lattice are dynamic and can compensate for temperature variations. Adjustments are possible because strut vertices are active through the use of piezo motors which can flex the entire structure to conform to the optical specification of λ/4 wavefront control. Such 6 degrees of freedom repositioning can be found in garden variety hexapods, Figure 66. These are routinely used on optical benches where nanometer resolution must be combined with great lifting capacity. Unlike a single hexapod, the DUET multiple joint latticework provides dozens of opportunities for kinematic control.

Fig 66 Hexapod with 6D movement

The trusses, as fully assembled, are shown in Figure 67. The attachment of the GZP by robotic spacecraft is illustrated in Figure 68. Truss assembly similarly is undertaken by robot teams which handle the structural tubes of Figure 66. With the structure joined at the receiver side in the back of the telescope, inner and outer trusses are joined at the primary objective location by pop-up stiffeners which are pre-integrated into the GZP mandrel. Piezo motors on the stiffener ribs tension the membrane during operation to maintain pitch tolerances to sub-wavelength accuracy across the 50 m annulus.

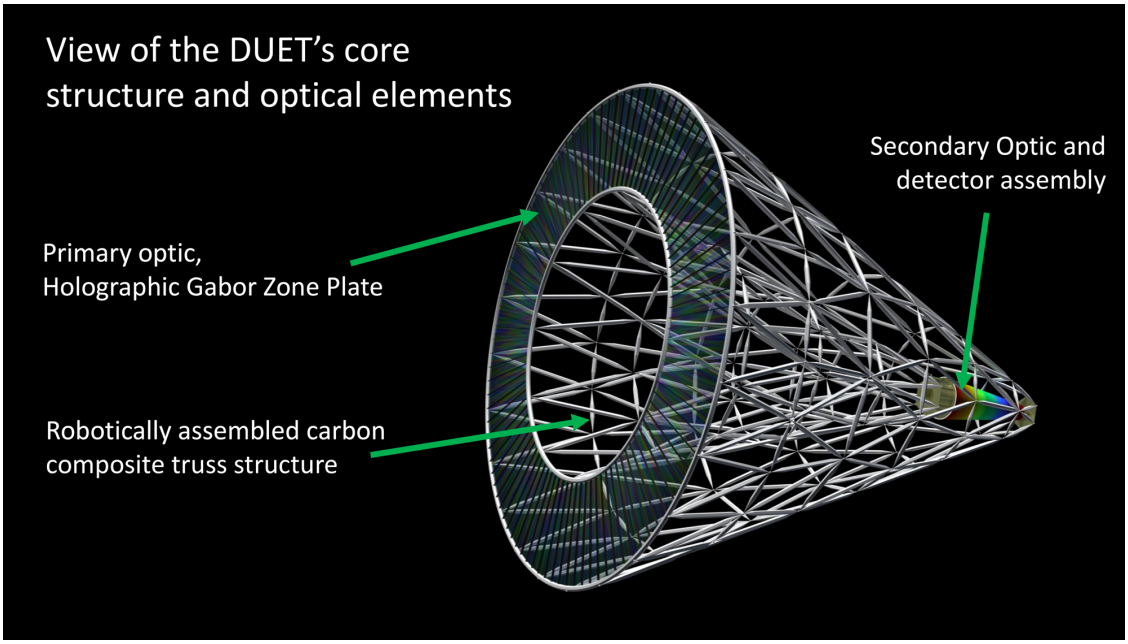

Fig. 67 Annotated Core Structure

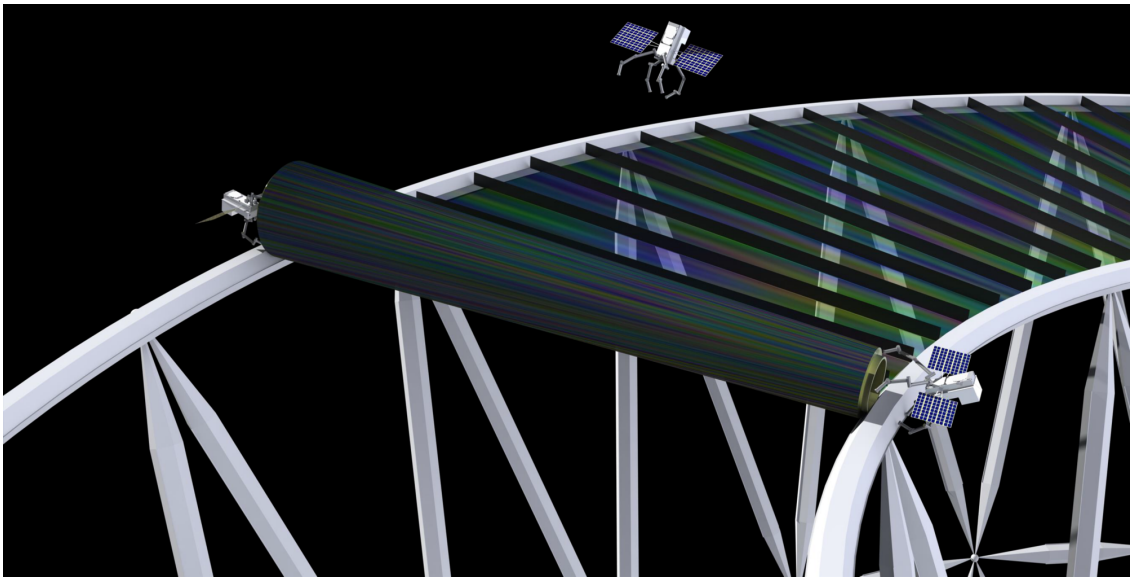

Fig 68 Team of 3 TUI spacecraft assemble tube structure and roll out the GZP and stiffeners.

The tunnel between the inner and outer diameter can be seen in Figures 69-70. This is not an unobscured wavefront, due to the stiffeners, but the secondary is segmented in-line with the ribs, avoiding unwanted diffraction artifacts in acquisition of the wavefront.

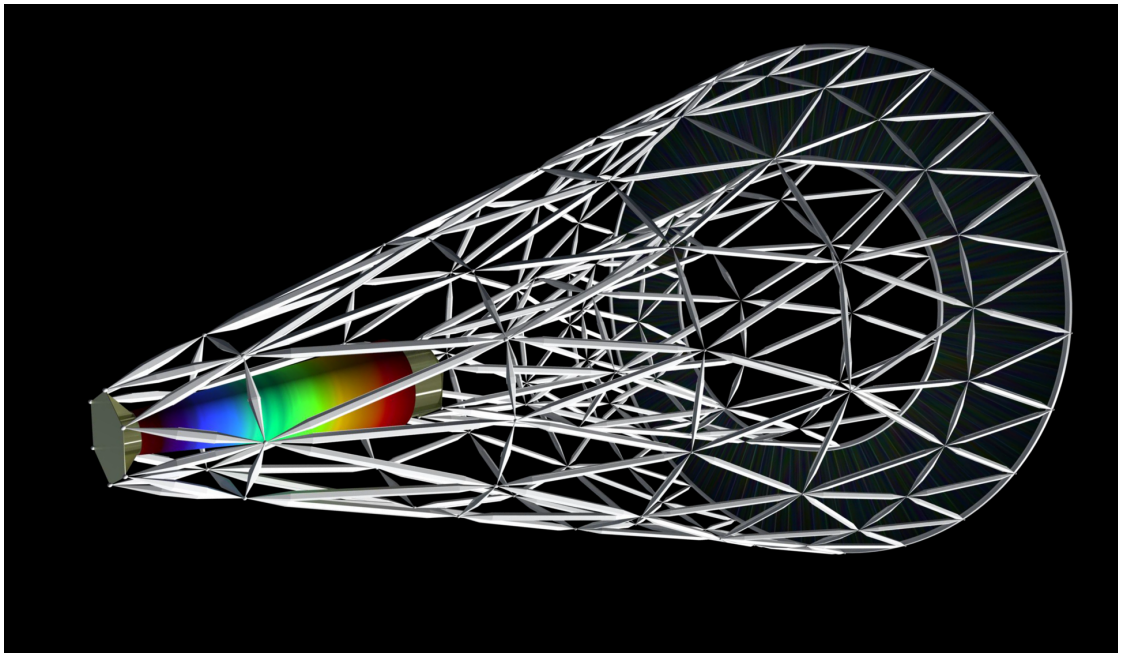

Fig. 69 View of DUET's core structure and optical elements prior to installing shades

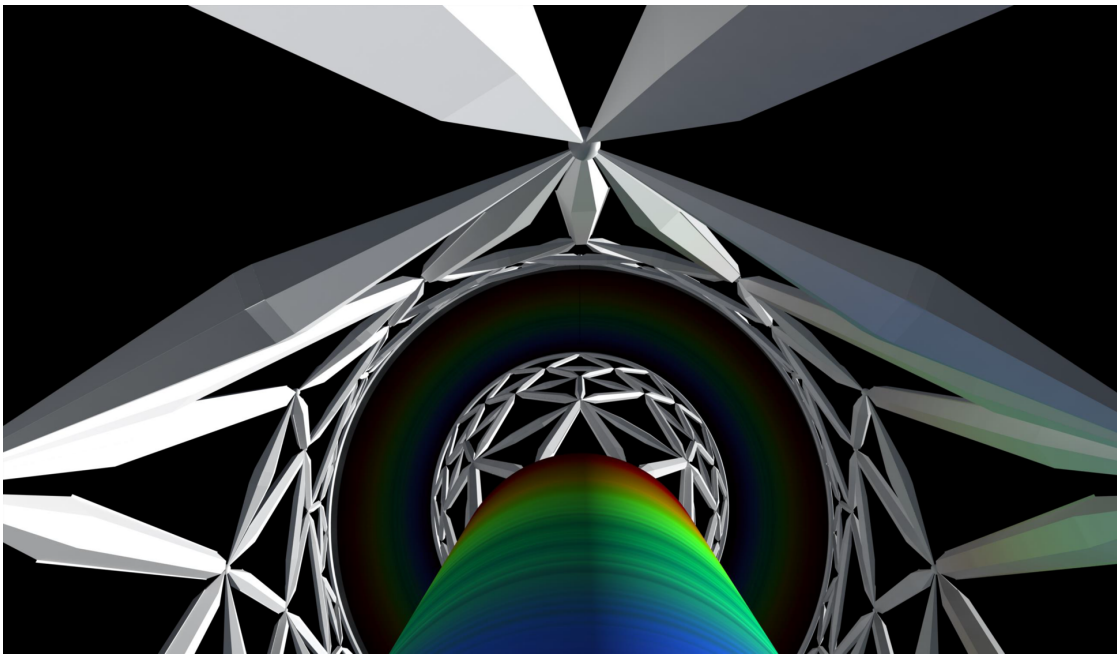

Fig. 70 Wide angle view from inside at secondary optic looking toward GZP

The addition of a sun shade and optics shades are illustrated in Figure 71.

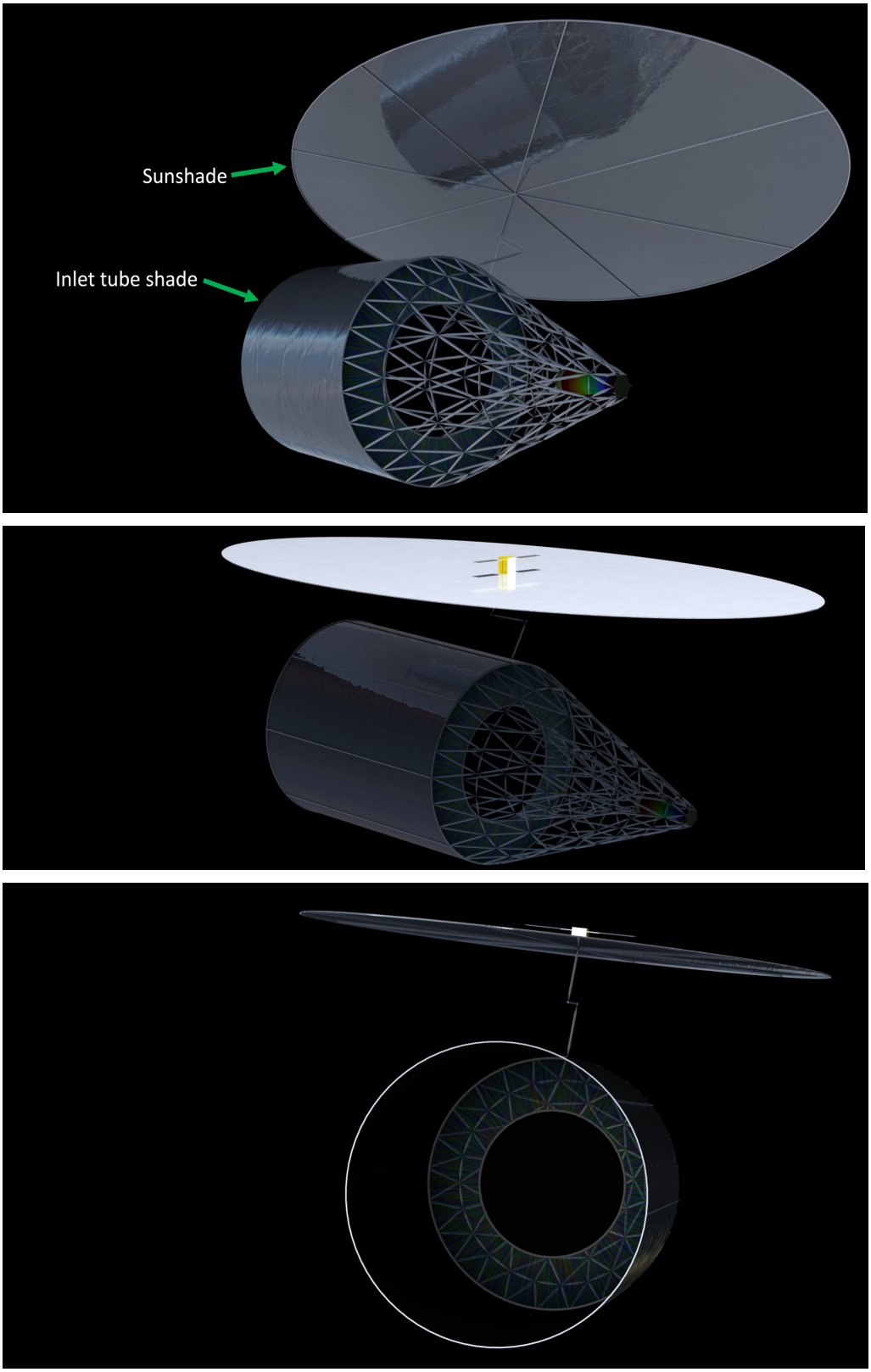

Fig. 71 Views with shades added

7. Conclusion and Recommendations for future work

DUET is the first POG telescope we have studied that exclusively uses diffractive elements in almost every optical train. It follows some 20 years of investigation into POG telescopes where mirrors and lenses were used. We have included some background on these in Sections 2 and 4, because this field is quite recent given the 400 year history of astronomical telescopes in refractive and reflective modes. Some readers of this report may be encountering the concept for the first time. This may be a revolutionary concept, so we employed evolutionary optics in earlier iterations with ribbon POGs.

We learned that an annulus configuration offers advantages over our prior linear ribbon POG telescopes. In exoplanet discoveries, an annulus potentially has a coronagraphic implementations that take advantage of chromatic separation and a circular secondary. It remains for us to continue the investigation to determine angular resolution on simulated exoplanetary systems. We do not know how multiple exoplanets or binary stars will interact with each other. We do not know if the overall aperture around the ring can be maintained in phase well enough to enjoy the benefit of DUET's considerable diameter. There is nothing in the physics that prohibits it, but we are skeptical about phase control.

We are confident that the ribbon optics, be they linear or annular, offer an enormous savings in areal mass over any prior primary objective. We remain confident that the surface flatness tolerance is highly relaxed compared to mirrors, but nothing is free. Where the flatness may be relaxed, the pitch precision is as demanding as a mirror figure, that is $\lambda/4$ or better. We are curious about the recently introduced flexible glasses such as Corning's Willow® glass. The company's Pyrex® made Palomar possible and Willow® may hold the key to DUET's success. We will speak to their researchers in confidence.

If there is a killer for our concept, it will be grating efficiency. If our Phase I GZP sets the limit (we measured 20%), it will barely suffice for faint objects, notwithstanding that the collector will be an order of magnitude greater in area than any telescope now in existence. However, it is not known if first-order efficiency is so limited. The example of VPHG's suggests to 50% efficiency is a reasonable expectation as the technology advances. The physics of gratings has not been fully written with regard to this parameter. Our Zemax models offer geometric proof that the telescope works, but that software does not answer the efficiency problem.

Recommended Phase II studies:

- Theory and practice of transmission GZP efficiency
- Holographic mastering methods for very large GZPs
- Earth 2.0 simulation identifying features detectable spectrographically
- Analog and digital methods for secondary receiver including sensor options
- Cornagraphs: ADI, Absorption Line Phasing; BLOC
- ConOps: Launch package and iSAT

Acknowledgements

Thanks to the RPI Department of Physics, Applied Physics and Astronomy, particularly to Professor Peter Persans whose facilities and guidance were instrumental in this project.

The GZP was fabricated in the RPI Nano-Photonics Laboratory of Dr. Shawn-Yu Lin. His equipment and moral support made this hologram possible.

REFERENCES

[1] Michel Mayor and Didier Queloz. Nobel Prize in Physics 2019 https://www.nobelprize.org/uploads/2019/10/advanced-physicsprize2019-3.pdf p.15 *ff*

[2] https://exoplanets.nasa.gov/exep/about/missions-instruments

[3] Dravins, Lindegren & Madsen, "Astrometric radial velocities. I. Non-spectroscopic methods for measuring stellar radial velocity," https://arxiv.org/abs/astro-ph/9907145v2, July 1999

[4] http://3dewitt.com/telescope/slide3

[5] David J. Erskine and Jerry Edelstein "High-Resolution Broadband Spectral Interferometry, "*Proc. SPIE 4854*, Astronomical Telescopes and Instrumentation, Aug. 2002

[6] http://www.recons.org/census.posted.htm

[7] https://arxiv.org/abs/1710.03775

[8] https://www.cfa.harvard.edu/MEarth/Welcome.html

[9] https://www.saintex.unibe.ch/

[10] https://en.wikipedia.org/wiki/Habitability_of_red_dwarf_systems

[11] https://iopscience.iop.org/article/10.3847/2041-8213/ab0651

[12] http://www.astrosurf.com/zodex/guide/CaK/CaK.html

[13] Howard A. MacEwen and James B. Breckinridge, "Large diffractive/refractive apertures for space and airborne telescopes," *Sensors and Systems for Space Applications VI*, *Proc. SPIE* 8739 (May 21, 2013); http://dx.doi.org/10.1117/12.2015457

[14] Travis Blake, "MORE Membrane Optic Image Real-Time Exploitation," DARPA *SeeMe Industry Day*, 27 March 2011 Slide 5, "Diffraction Telescope Challenges"

[15] Geoff Andersen, "Large optical photon sieve," *OPTICS LETTERS* / Vol. 30, No. 22 / November 15, 2005

[16] Geoff Andersen and Drew Tullson, "Broadband antihole photon sieve telescope," *Applied Optics*, Vol. 46, No. 18, 20 June 2007.

[17] Ditto, Friedman and Content, "Astronomical telescope with holographic primary objective," *Proc. SPIE* 8146, *UV/Optical/IR Space Telescopes and Instruments: Innovative Technologies and Concepts V*, 814615 (14 September 2011); doi: 10.1117/12.893141

[18] Yannick Copin, "Slitless spectro-photometry, LSST-DESC Calibration Workshop, Oct. 2018 https://indico.in2p3.fr/event/17773/contributions/65639/attachments/50164/63980/slitlessSpectroPhoto.pdf

[19] https://www.slideserve.com/raven-booth/hubble-s-slitless-spectroscopy

[20] Isaac Newton, *Opticks*, (4th ed 1730), p. 46, http://www.gutenberg.org/files/33504/33504-h/33504-h.htm "Exper. 6. In the middle of two thin Boards I made round holes a third part of an Inch in diameter, and in the Window-shut a much broader hole being made to let into my darkened Chamber a large Beam of the Sun's Light; I placed a Prism behind the Shut in that beam to refract it towards the opposite Wall, and close behind the Prism I fixed one of the Boards, in such manner that the middle of the refracted Light might pass through the hole made in it, and the rest be intercepted by the Board. Then at the distance of about twelve Feet from the first Board I fixed the other Board in such manner that the middle of the refracted Light which came through the hole in the first Board, and fell upon the opposite Wall, might pass through the hole in this other Board, and the rest being intercepted by the Board might paint upon it the coloured Spectrum of the Sun. And close behind this Board I fixed another Prism to refract the Light which came through the hole. Then I returned speedily to the first Prism, and by turning it slowly to and fro about its Axis, I caused the Image which fell upon the second Board to move up and down upon that Board, that all its parts might successively pass through the hole in that Board and fall upon the Prism behind it. And in the mean time, I noted the places on the opposite Wall to which that Light after its Refraction in the second Prism did pass; and by the difference of the places I found that the Light which being most refracted in the

first Prism did go to the blue end of the Image, was again more refracted in the second Prism than the Light which went to the red end of that Image, which proves as well the first Proposition as the second. And this happened whether the Axis of the two Prisms were parallel, or inclined to one another, and to the Horizon in any given Angles."

[21] http://3dewitt.com/telescope/slide1

[22] Thomas D. Ditto, "Conservation of etendue in a primary objective grating telescope," *Proc. SPIE* 9151, *Advances in Optical and Mechanical Technologies for Telescopes and Instrumentation*, 91515T (18 July 2014); https://doi.org/10.1117/12.2055510

[23] http://3dewitt.com/telescope/slide2

[24], *Exoplanet Science Strategy*, National Academies of Science, Engineering and Medicine, (2018), https://www.nap.edu/download/25187 p. 148 *ff*

[25] Beckwith et al, The Hubble Ultra Deep Field, https://arxiv.org/pdf/astro-ph/0607632.pdf

[26] Travis Blake, *op. cit.*

[27] Chnaglun Hou "Novel diffractive optical element: binary photon sieve," *Optical Engineering* 50(6), 068001 (June 2011)

[28] Erwin Loewen *et al*, *Diffraction Grating Handbook*, seventh ed., 2014, p. 32 *ff* https://www.researchgate.net/publication/308402069_Diffraction_Grating_Handbook_7th_edition

[29] Jordan Wachs, "Spectrally-Resolved Synthetic Imaging Interferometer," NIAC 2018 Phase I https://www.nasa.gov/directorates/spacetech/niac/2018_Phase_I_Phase_II/Spectrally-Resolved_Synthetic_Imaging_Interferometer

[30] https://ntrs.nasa.gov/archive/nasa/casi.ntrs.nasa.gov/20190000920.pdf, p. 33

[31] Marina von Steinkirch, "... Earthshine," http://astro.sunysb.edu/steinkirch/talks/poster_poster.pdf

[32] http://www.iup.uni-bremen.de/gome/gomeinst.html

[33] Paul Gilster, "ESO: Habitable Red Dwarf Planets Abundant," http://www.centauri-dreams.org/?p=22313

[34] "Tidal Lock...", http://physics.stackexchange.com/questions/12541/tidal-lock-radius-in-habitable-zones

[35] Gilles Durand, Marc Sauvage, Aymeric Bonnet, et al, TALC, a new deployable concept for a 20-m far-infrared space telescope, *Proc. of SPIE* Vol. 9143, 91431A (2014), doi: 10.1117/12.2055895

[36] NASA, https://www.eurekalert.org/multimedia/pub/120636.php

[37] Robert J. Collier, Christoph B. Burckhardt and Lawrence H. Lin, *Optical Holography*, Academic press, 1971, Chap. 3, Section 3.31 "In-line Hologram Images," p. 72

[38] Stephen P. McGrew, METHOD OF FABRICATING SURFACE RELIEF HOLOGRAMS, US Patent 4,758,2296, Jul. 19 1988 http://www.freepatentsonline.com/4758296.pdf

[39] Christian Thalman, http://www.mpia.de/homes/thalmann/adi.htm

[40] https://exoplanets.nasa.gov/search.html?q=TPF

[41] *Terrestrial Planet Finder Interferometer Science Working Group Report*, Lawson, Lay, Johnston; Beichman, editors, 2007, https://exoplanets.nasa.gov/files/exep/TPFIswgReport2007.pdf

[42] *TPF Coronagraph Flight Baseline 1 Design Interim Status Report*, Virginia Ford, editor, 2005 https://exoplanets.nasa.gov/files/exep/TPFC-FB1_Report.pdf

[43] Thomas D. Ditto, "Self-nulling spectrograph for star glare rejection," *Proc. SPIE* 11117, *Techniques and Instrumentation for Detection of Exoplanets IX*, 111171P (9 September 2019); https://doi.org/10.1117/12.2525524

[44] https://en.wikipedia.org/wiki/Daguerreotype

[45] http://www.litiholo.com/hologram-film.html

[46] https://litiholo.com/Litiholo%20CRT20%20hologram%20film%20spec%20sheet.pdf

[47] Chonis, et all, "Mass production of volume phase holographic gratings for the VIRUS spectrographic array, "arXiv:1407.7537v1 [astro-ph.IM] 28 Jul 2014

[48] https://wasatchphotonics.com/technologies/volume-phase-holographic-gratings/

[49]https://www.corning.com/media/worldwide/Innovation/documents/WillowGlass/Corning%20Willow%20Glass%20Fact%20Sheets_August2019.pdf

[50] Rudranarayan Mukherjeea, Nicholas Sieglerb; Harley Thronsonc, "The Future of Space Astronomy will be Built: Results from the In-Space Astronomical Telescope (iSAT) Assembly, Design Study," 70th International Astronautical Congress (IAC), Washington D.C., United States, 21-25 October 2019